C.P. No. 642

C.P. No. 642

MINISTRY OF AVIATION

AERONAUTICAL RESEARCH COUNCIL

CURRENT PAPERS

The Effect of Skin Taper on the Aeroelastic Properties of Wings

by

J. A. Rein

LONDON: HER MAJESTY'S STATIONERY OFFICE

1963

PRICE 5s 6d NET

U.D.C. No. 533.6.013.412 : 629.13.012.612

C.P. No.642

March, 1961

THE EFFECT OF SKIN TAPER ON THE AEROELASTIC PROPERTIES OF WINGS

by

J. A. Rein

SUMMARY

An analysis is made of the effect of linear variation of the spanwise skin thickness on the divergence, flutter, and aileron reversal speeds of thin wings.

It is assumed that the wing weight and stiffness are provided by the skin alone and that the wing mass remains constant for the tapers considered.

It is shown that for rectangular wings, a skin thickness tapering from root to tip produces an increase of up to 8% in the critical speeds, whereas an inverse taper results in a reduction of up to 14%. For a tapered wing, skin thickness tapering from root to tip results in a reduction in the critical speeds of up to 7%.

A comparison is made between the results obtained from the analysis and from some flutter speed criteria. Further the effect of skin taper on the mode of distortion and on the dynamic torsional stiffness is investigated.

Replaces R.A.E. Report No. Structures 264 - A.R.C. 22,983

LIST OF CONTENTS

LIST OF TABLES

LIST OF ILLUSTRATIONS

1 INTRODUCTION

In recent years there have been numerous reports[1,2,3] on the effect of wing taper on the various aspects of aeroelasticity. It was felt that there was a need to investigate the corresponding effect of varying the spanwise skin thickness.

The scope of the present investigation, with its concept of an idealised wing is (a) to show the effect of the different modes on the aeroelastic properties, (b) to make a comparison of the results obtained with various criteria in use at the R.A.E. to ascertain if a correction factor for skin taper is necessary, (c) to show the variation of the measured static stiffness to the effective dynamic stiffness for the various tapers taken over a range of reference sections.

The problem was approached by choosing a stiffness distribution along the span and obtaining where possible the exact solution for the modes of deformation. Where the exact solution could not readily be obtained simpler methods of calculation were used.

2 VARIATION OF WING PROPERTIES WITH TAPER

The geometry and basic properties of the wing are shown in Fig.1 and Table 1 respectively. These are similar to those used by Molyneux[4] but the flexural axis has been moved further aft to obtain a finite divergence speed.

The wing is considered to be a thin walled closed tube with constant wing thickness to chord ratio, the wing weight and stiffness being provided by the skin alone. To provide a basis for comparison of the effect of taper a constant wing mass was maintained. It is assumed that plane cross sections of the wing remain plane under load, and that the skin thickness and the wing chord vary spanwise in a linear manner.

With these assumptions it can be shown that taking the mean chord as standard we can express the skin thickness and the chord in the following manner,

$$t = \frac{2\,(1 - \Gamma\eta)\,t_r}{(2 - \Gamma)} \qquad (1)$$

$$c = \frac{2\,(1 - \tau\eta)\,c_m}{(2 - \tau)} \quad . \qquad (2)$$

If wing taper and skin taper are considered together then the skin thickness at the mean chord will have to be varied to keep the wing mass constant. If t_m is the skin thickness of a wing having uniform skin thickness it can be shown that for constant wing mass

$$t_r = \left\{1 - \frac{\tau\Gamma}{12 - 6\,(\tau + \Gamma) + 4\tau\Gamma}\right\} t_m \qquad (3)$$

Thus for a rectangular wing ($\tau = 0$) or constant skin thickness ($\Gamma = 0$) we have $t_r = t_m$.

From the Bredt-Batho formulae for a thin wall tube with parallel generators we have that the St. Venant torsion constant J is proportional to the skin thickness t.

For a rectangular wing the torsional rigidity at an arbitrary section is given by

$$GJ = \frac{2(1 - \Gamma\eta)}{(2 - \Gamma)} GJ_r \quad .$$

Taking wing taper into account we have

$$GJ = \left\{\frac{2(1 - \tau\eta)}{(2 - \tau)}\right\}^3 \frac{2(1 - \Gamma\eta)}{(2 - \Gamma)} GJ_r \qquad (4)$$

where

$$GJ_r = \left\{1 - \frac{\tau\Gamma}{12 - ((\tau + \Gamma) + 4\tau\Gamma}\right\} GJ_m \quad .$$

Similarly for local value of the inertia

$$I = \left\{\frac{2(1 - \tau\eta)}{(2 - \tau)}\right\}^3 \frac{2(1 - \Gamma\eta)}{(2 - \Gamma)} I_r \quad . \qquad (5)$$

There are four cases for which solutions can be readily obtained:-

(a) $\tau = \Gamma = 0$ Rectangular wing with uniform skin

(b) $\tau = 0$ $\Gamma \neq 0$ Rectangular wing with skin taper

(c) $\tau \neq 0$ $\Gamma = 0$ Tapered wing with uniform skin

(d) $\tau = \Gamma \neq 0$ Tapered wing with same value for skin taper.

The tapers considered are:-

$\Gamma = 0, 1, 2/3, -2$ so that $\frac{t_T}{t_R} = 1, 0, 1/3, 3$ respectively and

$\tau = 0, 2/3$ so that $\frac{C_T}{C_R} = 1, 1/3.$

3 DIVERGENCE

The method used for the solution of the problem of wing torsional divergence is essentially that outlined by Broadbent[3]. The wing is considered to be rigidly built-in at the root, while the aerodynamic coefficient a_1 is assumed to be constant along the span and independent of the twist of the wing. Considering the wing to be a tube in which the skin thickness can be varied spanwise the position of the flexural axis will be constant chordwise and taking the aerodynamic centre at the $\frac{1}{4}$ chord position we have the parameter e constant.

The general differential equation is developed for wing and skin taper, and then the 'exact' solution, for the different cases, is found.

3.1 Derivation of equation

For the critical condition we have $\frac{d\theta}{dy} = \frac{1}{2}\frac{\rho V^2}{GJ}\int_y^s e\, a_1\, c^2\, \theta\, dy$

or

$$\theta = \tfrac{1}{2}\rho V^2 \int_0^y \frac{1}{GJ}\int_y^s e\, a_1\, c^2\, \theta\, dy\, dy \quad . \tag{6}$$

Substituting equations (2) and (4) into the above and writing

$\frac{Y}{s} = \eta$ and $\theta = \theta_o f(y)$

$$f = \rho V^2 \frac{(2-\tau)(2-\Gamma)\, e\, a_1}{8\, GJ_r}\, c_m^2\, s^2 \int_0^\eta \frac{1}{(1-\tau\eta)^3(1-\Gamma\eta)}\int_\eta^1 (1-\tau\eta)^2 f\, d\eta\, d\eta \quad . \tag{7}$$

Putting

$$u^2 = \rho V^2 \frac{(2-\tau)(2-\Gamma)\, e\, a_1}{8\, GJ_r}\, c_m^2\, s^2 \tag{8}$$

and differentiating (7) we obtain

$$\frac{df}{d\eta} = \frac{u^2}{(1-\tau\eta)^3\,(1-\Gamma\eta)}\int_\eta^1 (1-\tau\eta)^2 f\, d\eta \quad .$$

Further differentiating then yields

$$(1-\tau\eta)^3\,(1-\Gamma\eta)\frac{d^2f}{d\eta^2} - (1-\tau\eta)^2\left\{3\tau(1-\Gamma\eta) + \Gamma(1-\tau\eta)\right\}\frac{df}{d\eta} = -u^2(1-\tau\eta)^2 f \quad .$$

If $(1-\tau\eta) \neq 0$,

$$(1-\tau\eta)(1-\Gamma\eta)\frac{d^2f}{d\eta^2} - \left\{3\tau(1-\Gamma\eta) + \Gamma(1-\tau\eta)\right\}\frac{df}{d\eta} + u^2 f = 0 \tag{9}$$

3.2 Solutions for particular cases

(a) $\tau = \Gamma = 0$, rectangular wing with uniform skin thickness. Equation (9) reduces to

$$\frac{d^2f}{d\eta^2} + u^2 f = 0 \quad . \tag{10}$$

Solution of this equation is of the form

$$f = A \sin u\eta + B \cos u\eta$$

where A and B are arbitrary constants defined by the boundary conditions which are $f = 0$ when $\eta = 0$ and $\frac{df}{d\eta} = 0$ when $\eta = 1$.

Therefore

$$B = 0 \quad \text{and} \quad Au\cos u = 0$$

whence since

$$A \neq 0, \qquad u = (2n + 1)\frac{\pi}{2}, \; n = 0, 1, 2 \ldots.$$

For the lowest critical speed from equation (8) with $n = 0$ we have

$$V = \frac{\pi}{2}\sqrt{\frac{2\,GJ_r}{\rho e a_1 s^2 c_m^2}} \quad .$$

(b) $\tau = 0$ $\Gamma \neq 0$, rectangular wing with varying skin thickness. Equation (9) reduces to

$$(1 - \Gamma\eta)\frac{d^2f}{d\eta^2} - \Gamma\frac{df}{d\eta} + u^2 f = 0 \quad . \tag{11}$$

By substituting $(1 - \Gamma\eta) = \xi$ equation (11) can be modified to a form of Bessel's equation expressed as

$$\frac{d^2f}{d\xi^2} + \frac{1}{\xi}\frac{df}{d\xi} + \frac{1}{\xi}\frac{u^2}{\Gamma^2} f = 0 \quad .$$

The solution of which is

$$f = AJ_o\left(2\frac{u}{\Gamma}\sqrt{1 - \Gamma\eta}\right) + BY_o\left(2\frac{u}{\Gamma}\sqrt{1 - \Gamma\eta}\right) \tag{12}$$

where A and B are arbitrary constants and J,Y refer to the appropriate Bessel functions. Applying the boundary conditions $f = 0$ when $\eta = 0$ and $df/d\eta = 0$ when $\eta = 1$ we obtain two equations of the form

$$AJ_o\left(2\frac{u}{\Gamma}\right) + BY_o\left(2\frac{u}{\Gamma}\right) = 0$$

$$AJ_1\left(2\frac{u}{\Gamma}\sqrt{1 - \Gamma}\right) + BY_1\left(2\frac{u}{\Gamma}\sqrt{1 - \Gamma}\right) = 0$$

from which the lowest critical speed which satisfies both equations simultaneously for a particular value of Γ can be found. Details of a graphical method of obtaining the lowest critical speed and the mode of deformation is given in the Appendix.

(c) $\tau \neq 0$, $\Gamma = 0$. Equation (9) for a tapered wing with uniform skin thickness reduces to

$$(1 - \tau\eta) \frac{d^2f}{d\eta^2} - 3\tau \frac{df}{d\eta} + u^2 f = 0 \quad . \tag{13}$$

Making the substitution $(1 - \tau\eta) = \zeta$ it can be verified that equation (13) reduces to a Bessel equation of the form

$$\frac{d^2f}{d\zeta^2} + \frac{3}{\zeta} \frac{df}{d\zeta} + \frac{1}{\zeta} \frac{u^2}{\tau^2} f = 0 \quad .$$

The solution of which is

$$f = (1 - \tau\eta)^{-1} \left\{ AJ_2 \left(2 \frac{u}{\tau} \sqrt{1 - \tau\eta}\right) + BY_2 \left(2 \frac{u}{\tau} \sqrt{1 - \tau\eta}\right) \right\} \quad . \tag{14}$$

Substituting in the boundary condition and by a method similar to 3.2(b) and the Appendix the lowest critical speed and corresponding mode of deformation is found.

(d) $\tau = \Gamma \neq 0$, for a tapered wing with the same skin taper equation (9) reduces to

$$(1 - \tau\eta)^2 \frac{d^2f}{d\eta^2} - 4\tau (1 - \tau\eta) \frac{df}{d\eta} + u^2 f = 0$$

the solution of which[3] is

$$f = (1 - \tau\eta)^{-3/2} \left[A \sin \left\{ \alpha \log(1 - \tau\eta) \right\} + B \cos \left\{ \alpha \log(1 - \tau\eta) \right\} \right]$$

where

$$\alpha = \left\{ \left(\frac{u}{\tau}\right)^2 - \frac{9}{4} \right\}^{1/2} \quad . \tag{15}$$

Satisfying the boundary conditions we have for $\eta = 0$, $B = 0$, and $\eta = 1$,

$$\alpha = \frac{3}{2} \tan \left\{ \alpha \log (1 - \tau) \right\} \tag{16}$$

(since $A \neq 0$).

Solving this equation for α in terms of τ we obtain the critical divergence speed by substitution from equations (8) and (13).

3.3 Numerical examples

With the substitution of the taper values in section 2, and the wing properties, listed in Table 1, into the solutions of the differential equations, the divergence speeds are obtained, shown in Table 2, and the divergence mode shapes are as shown in Fig.2. The ratio of the divergence speed with taper to the divergence speed of the rectangular wing with uniform skin thickness is plotted against the value of the skin taper in Fig.6. This shows that for a rectangular wing of constant mass the divergence speed increases with skin taper, whereas for a tapered wing of constant mass the divergence speed decreases with increasing skin taper for the range of skin taper $0 \leq \Gamma \leq 2/3$.

For the tapered wing the effect of keeping a constant skin thickness at the mean chord (rather than constant wing mass) is shown by the dotted line in Fig.6 and it can be seen that the divergence speed then increases with skin taper. However, comparison for constant mass seems more logical, and on this basis it may be expected that there will be an initial increase of divergence speed as the value of the skin taper is reduced below $\Gamma = 0$. The probable result is shown by the broken line in Fig.6.

4 FLUTTER

For the flutter investigation, only two modes were considered, namely, pure flexure and torsion about a flexure axis for a cantilever beam. The "exact" solution was obtained for the torsion mode but a simpler but slightly less accurate solution was obtained for the flexural mode, as it has been shown[1] that small variations in the flexural mode do not significantly affect the flutter mode.

4.1 Fundamental torsional mode

The differential equation is derived on the basis that the fundamental torsional mode of the wing in the flutter oscillation will be essentially the same as the fundamental torsional mode of a cantilever beam vibrating in vacuo. The justification of this assumption has been demonstrated[1,5].

4.1.1 Derivation of equation

The method used is essentially that developed in Refs.1,6,7. The differential equation for the torsional oscillation of the wing is

$$I \frac{\partial^2 \theta}{\partial t^2} - \frac{\partial}{\partial y}\left(GJ \frac{\partial \theta}{\partial y}\right) = 0 \quad . \qquad (17)$$

For the fundamental mode of vibration

$$\theta = \theta_1 \sin (pt + \varepsilon) \quad \text{or} \quad \frac{\partial^2 \theta}{\partial t^2} = - p^2 \theta \quad .$$

Substituting equations (4) and (5) into equation (17) and changing the variable we have

$$\frac{GJ_r}{s^2}\ \frac{d}{d\eta}\left\{(1-\tau\eta)^3\ (1-\Gamma\eta)\ \frac{d\theta}{d\eta}\right\} + p^2\ I_r\ (1-\tau\eta)^3\ (1-\Gamma\eta)\ \theta\ =\ 0 \qquad \ldots\ (18)$$

performing the differentiations and if $(1-\tau\eta) \neq 0$ we can write

$$(1-\tau\eta)(1-\Gamma\eta)\ \frac{d^2\theta}{d\eta^2} - \left\{3\tau(1-\Gamma\eta) + \Gamma(1-\tau\eta)\right\}\frac{d\theta}{d\eta} + K^2(1-\tau\eta)(1-\Gamma\eta)\,\theta\ =\ 0 \qquad \ldots\ (19)$$

where

$$K^2\ =\ \frac{p^2\ s^2\ I_r}{GJ_r} \qquad (20)$$

4.1.2 Solutions for particular cases

(a) $\tau = \Gamma = 0$

The differential equation (19) reduces to

$$\frac{d^2\theta}{d\eta^2} + K^2\theta\ =\ 0\ . \qquad (21)$$

The solution of which is

$$\theta\ =\ A \sin K\eta + B \cos K\eta$$

where A and B are arbitrary constants. Applying the end conditions (i) $\theta = 0$ where $\eta = 0$ and (ii) $d\theta/d\eta = 0$ when $\eta = 1$ we have from (i) that $B = 0$ and from (ii) that since $A \neq 0$, $\cos K = 0$, or $K = (2n + 1)\ \pi/2$ $n = 0, 1, 2$. Therefore

$$p\ =\ \frac{\pi}{2s}\sqrt{\frac{GJ_r}{I_r}}\ . \qquad (22)$$

It is assumed that the frequency of torsional vibration of the rectangular wing with constant skin thickness is 50 c.p.s. Hence we obtain the value of the torsional rigidity, and the mode of oscillation is given by

$$\theta\ =\ A \sin\frac{\pi}{2}\eta \qquad (23)$$

where A is to be determined by the amplitude of the oscillation.

(b) $\tau = 0,\ \Gamma \neq 0$

The differential equation (19) becomes,

$$(1 - \Gamma\eta)\frac{d^2\theta}{d\eta^2} - \Gamma\frac{d\theta}{d\eta} + K^2(1 - \Gamma\eta)\theta = 0 \quad .$$

Putting $(1 - \Gamma\eta) = \zeta$ this equation can be reduced to a Bessel equation of the form

$$\frac{d^2\theta}{d\zeta^2} + \frac{1}{\zeta}\frac{d\theta}{d\zeta} + \frac{K^2}{\Gamma^2}\theta = 0 \quad .$$

The solution of which is

$$\theta = AJ_o\left\{\frac{K}{\Gamma}(1 - \Gamma\eta)\right\} + BY_o\left\{\frac{K}{\Gamma}(1 - \Gamma\eta)\right\} \qquad (24)$$

where A and B are arbitrary constants and J refers to the appropriate Bessel functions. Applying the end conditions (i) $\theta = 0$ when $\eta = 0$ (ii) $d\theta/d\eta = 0$ when $\eta = 1$ we obtain two equations of a form similar to those of sect. 3.2(b) and by use of the same method we obtain the fundamental torsional frequency, and the appropriate mode.

(c) $\tau \neq 0,\ \Gamma = 0$

Equation (19) becomes

$$(1 - \tau\eta)\frac{d^2\theta}{d\eta^2} - 3\tau\frac{d\theta}{d\eta} + K^2(1 - \tau\eta)\theta = 0 \quad .$$

This can also be modified to a form of the Bessel equation the solution of which is

$$\theta = (1 - \tau\eta)^{-1}\left\{AJ_1\left(\frac{K}{\tau}(1 - \tau\eta)\right) + BY_1\left(\frac{K}{\tau}(1 - \tau\eta)\right)\right\} \qquad (25)$$

where A, B are arbitrary constants and J, Y refer to the appropriate Bessel functions. By a similar process to 3.2(b) the fundamental torsional frequency and associated mode are obtained.

(d) $\tau = \Gamma \neq 0$

Equation (19) reduces to

$$(1 - \tau\eta)^2\frac{d^2\theta}{d\eta^2} - 4\tau(1 - \tau\eta)\frac{d\theta}{d\eta} + K^2(1 - \tau\eta)^2\theta = 0 \quad .$$

This is the same form as equation (A.5)[1]. Reducing the equation to a form of the Bessel equation by substituting $(1 - \tau\eta) = \zeta$ we get

$$\frac{d^2\theta}{d\zeta^2} + \frac{4}{\zeta}\frac{d\theta}{d\zeta} + \frac{K^2}{\tau^2}\theta = 0 \quad .$$

The solution of which is in the form

$$\theta = (1-\tau\eta)^{-3/2}\left\{AJ_{3/2}\left(\frac{K}{\tau}(1-\tau\eta)\right) + BJ_{-3/2}\left(\frac{K}{\tau}(1-\tau\eta)\right)\right\}. \qquad (26)$$

This may be written as a simple trigonometrical expression and the solution is then

$$\theta = (1-\tau\eta)^{-3}\,\beta^{-3/2}\left[A\left\{\sin\beta(1-\tau\eta) - \beta(1-\tau\eta)\cos\beta(1-\tau\eta)\right\} + B\left\{-\beta(1-\tau\eta)\sin\beta(1-\tau\eta) - \cos\beta(1-\tau\eta)\right\}\right].$$

This is compatible with equation (A.8)[1] and it is shown by satisfying the end conditions that the equation reduces to -

$$\beta^{1/2}(1-\tau\eta)^2\left(\frac{\theta}{A}\right) = \left\{\frac{\sin\beta(1-\tau\eta)}{\beta(1-\tau\eta)} - \cos\beta(1-\tau\eta)\right\} - \alpha\left\{\sin\beta(1-\tau\eta) + \frac{\cos\beta(1-\tau\eta)}{\beta(1-\tau\eta)}\right\}$$

where $\alpha = \dfrac{\sin\beta - \beta\cos\beta}{\beta\sin\beta + \cos\beta}$ and $\tan\beta = \dfrac{\beta\{3\tau-\beta^2(1-\tau)^2\}}{3+\beta^2(2+\tau)(1-\tau)}$

β is defined as the positive root of the expression

$$\beta^2 = \frac{s^2p^2}{\tau^2}\frac{I_r}{GJ_r} = \frac{s^2p^2}{\tau^2}\frac{I_m}{GJ_m} = \frac{K^2}{\tau^2}$$

whence the frequency p is given by

$$p = \frac{\tau\beta}{s}\left(\frac{GJ_m}{I_m}\right)^{1/2}.$$

4.1.3 Numerical examples

The frequencies are listed in Table 2 and the torsional modes are shown in Fig.3. The flutter coefficients were evaluated from the modes using Simpson's Rule.

4.2 Fundamental flexural mode

The fundamental flexural mode was calculated by treating the wing as a cantilever beam divided into four discrete sections. A comparison with the "exact" solution was obtained for case (a) and the mode shape and

frequency gave good agreement. The accuracy could be improved by increasing the number of sections. For case (a) ($\tau = \Gamma = 0$) the exact solution is

$$p = 2\pi f = \frac{1.875^2}{s^2}\sqrt{\frac{EI_m}{m}} \text{ rad/sec} .$$

A value of EI_m is thus obtained for the assumed frequency of 16 c.p.s.

4.2.1 Numerical examples

The results of the calculations are shown in Fig.4 and Table 2. A mode of parabolic shape of the form $z = \eta^2$ has been included in Fig.4 and it may be seen that it corresponds very closely to that of case (d) ($\tau = \Gamma = 2/3$). The modes and frequencies were used directly in the flutter calculations, Simpson's Rule being used in the evaluation of the flutter integrals.

4.3 Flutter calculations

The basis of the wing flexure - torsion flutter calculations is the method described by Templeton[8].

Two-dimensional incompressible flow aerodynamic derivatives[9] were used throughout as we are mainly interested in a comparison of the ratio of the flutter speeds and not an absolute value. Agreement was reached between the assumed and derived frequency parameter.

4.3.1 Numerical examples

The results obtained from the flutter calculations are listed in Table 2, and shown in Fig.7. In all cases the flutter speed and frequency are expressed as ratios of the speed and frequency of the wing with taper to that of the rectangular wing with constant skin thickness ($\tau = \Gamma = 0$).

It is seen that for the rectangular wing the flutter speed increases from a minimum value for inverse skin taper ($\Gamma = -2$) to a maximum for skin taper slightly < 1 then decreases. For the tapered wing with constant wing density, the flutter speed decreases with an increase in the skin taper in the range $0 \leqslant \Gamma \leqslant 2/3$. For skin taper < 0 an initial increase in the flutter speed seems likely. The probable result is shown by the broken line in Fig.7.

5 AILERON REVERSAL

The method adopted for obtaining the critical aileron reversal speed and associated mode is described in detail in R & M 2186 [2].

The integral equation is obtained and then the wing is divided into a number of rigid fore and aft strips interconnected by springs representative of the local stiffness. The solution then takes the form of an iterative process.

A half span aileron, extending to the wing tip, with ratio of aileron chord to wing chord E = 0.20 was used in the calculations. The appropriate aerodynamic data were determined from the geometry of the wing and aileron, and were assumed to be independent of the wing twist. Thus a_1 was taken to be constant over the wing span, and a_2 and m constant over the aileron span.

5.1 Derivation of equation

At the critical aileron reversal speed the equation developed in R & M 2186 [2] is of the form

$$f(y) = \frac{1}{2}\rho V^2 \int_0^y \frac{1}{GJ} \int_y^s c^2 \left[ea_1 f + (ea_2 - m) \left\{ 1 - f - \frac{A(f)}{C} \right\} \right] dy\, dy \quad \ldots \quad (27)$$

where

$$\theta = \theta_0 f(y)$$

$$A(f) = \int_0^s cy \left\{ (a_1 - a_2) f(y) + a_2 \right\} dy$$

$$C = \int_0^s a_2\, cy\, dy \quad .$$

The iteration process yields the aileron reversal speed and mode to a high order of accuracy.

5.2 Numerical examples

In all cases the critical aileron reversal speeds shown in Fig.8 are expressed as ratios to the critical speed of the rectangular wing with uniform skin thickness; the actual speeds obtained from the calculations are listed in Table 2. The modes obtained with the mid-aileron position as the reference section are as shown in Fig.5. It may be seen that the variation of aileron reversal speed with skin taper exhibits characteristics similar to the divergence speed results, having an increase in the critical speed for rectangular wings, with increase in skin taper. For the tapered wing in the range $0 \leqslant \Gamma \leqslant 2/3$ there is a reduction in the critical speed with increase in skin taper. The probable result for skin taper < 0 is shown by the broken line in Fig.8. In Fig.10 are shown the static torsional modes used in the iteration process obtained by applying a unit torque at the wing tip.

6 COMPARISON OF CALCULATED FLUTTER SPEEDS WITH CRITERION RESULTS

Two forms of criterion are in current use for predicting wing flutter. It is of interest to compare the speeds given by these criteria with the flutter speeds found in Section 4.

The criterion suggested by Molyneux[10] is based essentially upon the static stiffnesses of the wing. It is a semi-empirical criterion, developed using the results of wind tunnel and ground launched rocket model tests, and takes the following form:-

$$V_1 = \left(\frac{m_\theta}{\rho s\, c_m^2}\right)^{1/2} \frac{(0.9 - 0.33K)\left(0.77 + \frac{0.1}{r}\right)\left(0.95 + \frac{1.3}{\sigma_w}\right) \sec^{3/2}\left(\Lambda - \frac{\pi}{16}\right)}{0.78\,(g - 0.1)} \quad \ldots (28)$$

$$V_2 = V_1\,(1 - 0.166\, M_1 \cos \Lambda)$$

where V_2 is the required flutter speed.

Broadbent has proposed certain modifications to the above formula[11], the main feature being the use of the strain energy in a linear twist mode as an alternative to wing static torsional stiffness. The criterion is in a form suitable for early project work, and indicates the minimum stiffness required to give a safe margin on flutter at the design diving speed, thus

$$U = 0.0035\, s\, c^2\, V_D^2 \left\{ \frac{g \cos^{1/2} \beta}{\left(0.77 + \frac{0.1}{r}\right) \sec^{3/2}\left(\Lambda - \frac{\pi}{16}\right)(1 - 0.166M \cos \Lambda)} \right\}^{1/2} \quad \ldots (29)$$

where $M \cos \Lambda \leqslant 1$.

c is the chord (ft) at 0.75s from the root for $0 \leqslant \tau < 0.6$, or at $(0.775 - 0.125\,\tau)s$ from the root if $0.6 < \tau \leqslant 1.0$. β is the sweepback of the centre line of the box.

For low aspect ratio ($AR < 3$) replace $\sec^{3/2}\left(\Lambda - \frac{\pi}{16}\right)$ by $0.9\left\{1 + \frac{0.8}{A}\right\} \sec\left(\Lambda - \frac{\pi}{16}\right)$.

Since the formula includes a safety factor it cannot be used directly to predict flutter speed. It is therefore assumed that the flutter speed V_F is related to the speed V_D given by the formula, as follows:-

$$V_F = 1.25\, V_D \frac{(1 - 0.166 \times 1.25\, M_D)}{(1 - 0.166\, M_D)}$$

where M_D is the Mach number at speed V_D. The correction implies that the flutter speed is 25% higher than the design diving speed (roughly equivalent to a 50% margin on stiffness) and also allows for the change in Mach number.

The flutter speeds in Section 4 were found using aerodynamic derivatives for two-dimensional incompressible flow. In order to compare these speeds directly with those given by the criteria an allowance should be made for the effects of aspect ratio and Mach number. The following correction was adopted,

$$V = V_o \left(1 + \frac{0.8}{A}\right)(1 - 0.166\, M_o) ,$$

where V_o is the original calculated speed, and M_o the corresponding Mach number. No allowance is made for the leading edge sweepback of the tapered wing as its effect is small.

The criterion speeds and modified calculated speeds are given in Table 3. Each speed has been divided by the modified calculated speed for the rectangular wing with uniform skin thickness, and plotted as a speed ratio in Fig.9. The trends of variation of the modified calculated speeds with skin taper agree very well with those predicted by the Molyneux criterion, and the speeds are in excellent agreement for the rectangular wing. The corresponding trends predicted by the Broadbent criterion are opposite to those given by the Molyneux criterion and by calculation. It should be noted, however, that the variation of speed with skin taper is small in the range considered.

7 VARIATION OF TORSIONAL STIFFNESS WITH SKIN TAPER

The torsional stiffness of a wing as measured in a stiffness test at a reference section (static stiffness) will in general be different from the effective stiffness in the actual mode of deformation (dynamic stiffness). In Ref.1 an estimate has been made of the magnitude of this difference for the torsional mode in the flutter oscillation for tapered wings. In the present report the method is extended to include the effects of skin taper.

The problem is approached by considering the strain energy in the two modes for a range of reference sections. One mode, corresponding to the dynamic mode, is the "exact" mode obtained in Section 4.1 and the other is that appropriate to a concentrated torque applied at a reference section.

7.1 Static stiffness

The strain energy in the wing is derived from the general equation

$$dU = \frac{1}{2} \frac{GJ}{s} \left(\frac{d\theta}{d\eta}\right)^2 d\eta \quad . \tag{30}$$

If the concentrated torque is applied at some reference section η_o the static strain energy for the general problem can be written

$$U_s = \frac{1}{2} \frac{GJ_r\, 2^4}{s(2-\tau)^3(2-\Gamma)} \int_o^{\eta_o} (1-\tau\eta)^3(1-\Gamma\eta) \left(\frac{d\theta}{d\eta}\right)^2 d\eta \quad . \tag{31}$$

The static mode is given by

$$\theta \propto \frac{(2-\tau)^3\,(2-\Gamma)}{2^4\, GJ_r} \int_o^{\eta} \frac{d\eta}{(1-\tau\eta)^3\,(1-\Gamma\eta)}$$

and since by definition $\theta = \theta_o$ when $\eta = \eta_o$ where θ_o is the twist at the reference section we have

$$\theta = \frac{\theta_o \int_o^{\eta} \frac{d\eta}{(1-\tau\eta)^3 (1-\Gamma\eta)}}{\int_o^{\eta_o} \frac{d\eta}{(1-\tau\eta)^3 (1-\Gamma\eta)}} \tag{32}$$

Case (a) $\tau = \Gamma = 0$ Rectangular wing with uniform skin thickness

$$U_s = \frac{GJ_m}{2s} \int_o^{\eta_o} \left(\frac{d\theta}{d\eta}\right)^2 d\eta$$

$$= \frac{GJ_m}{2s} \frac{\theta_o^2}{\eta_o} \tag{33}$$

Case (b) $\tau = 0$, $\Gamma \neq 0$ Rectangular wing with skin taper

$$\theta = \theta_o \frac{\log(1-\Gamma\eta)}{\log(1-\Gamma\eta_o)}, \quad \frac{d\theta}{d\eta} = \frac{\theta_o}{\log(1-\Gamma\eta_o)} \cdot \frac{(-\Gamma)}{(1-\Gamma\eta)}$$

$$U_s = \frac{GJ_m}{s(2-\Gamma)} \frac{\theta_o^2 \Gamma^2}{\{\log(1-\Gamma\eta_o)\}^2} \int_o^{\eta_o} \frac{d\eta}{(1-\Gamma\eta)}$$

$$= -\frac{GJ_m}{s(2-\Gamma)} \cdot \frac{\theta_o^2 \Gamma}{\log(1-\Gamma\eta_o)} \tag{34}$$

/Case (c)

Case (c) $\tau \neq 0$, $\Gamma = 0$ Tapered wing with uniform skin thickness

$$\theta = \frac{\theta_o (1 - \tau\eta_o)^2}{1 - (1 - \tau\eta_o)^2} \left\{\frac{1 - (1 - \tau\eta)^2}{(1 - \tau\eta)^2}\right\}$$

$$\frac{d\theta}{d\eta} = \frac{\theta_o (1 - \tau\eta_o)^2}{1 - (1 - \tau\eta_o)^2} \cdot \frac{2\tau}{(1 - \tau\eta)^3}$$

$$U_s = \frac{16\, GJ_m}{s(2 - \tau)^3} \theta_o^2 \tau^2 \left\{\frac{(1 - \tau\eta_o)^2}{1 - (1 - \tau\eta_o)^2}\right\}^2 \int_o^{\eta_o} \frac{d\eta}{(1 - \tau\eta)^3}$$

$$= \frac{8\, GJ_m \tau}{s(2 - \tau)^3} \theta_o^2 \left\{\frac{(1 - \tau\eta_o)^2}{1 - (1 - \tau\eta_o)^2}\right\} \qquad (35)$$

Case (d) $\tau = \Gamma \neq 0$

$$\theta = \frac{\theta_o (1 - \tau\eta_o)^3}{\{1 - (1 - \tau\eta_o)^3\}} \left\{\frac{1 - (1 - \tau\eta)^3}{(1 - \tau\eta)^3}\right\}$$

$$\frac{d\theta}{d\eta} = \theta_o \left\{\frac{(1 - \tau\eta_o)^3}{1 - (1 - \tau\eta_o)^3}\right\} \frac{3\tau}{(1 - \tau\eta)^4}$$

therefore

$$U_s = \frac{8\, GJ_r}{s(2 - \tau)^4} \theta_o^2 \left\{\frac{(1 - \tau\eta_o)^3\, 3\tau}{1 - (1 - \tau\eta_o)^3}\right\}^2 \int_o^{\eta_o} \frac{d\eta}{(1 - \tau\eta)^4}$$

$$= \frac{24\, GJ_r}{s(2 - \tau)^4} \tau\theta_o^2 \left\{\frac{(1 - \tau\eta_o)^3}{1 - (1 - \tau\eta_o)^3}\right\} . \qquad (36)$$

7.2 Dynamic stiffness

As before the strain energy in the wing is derived from the general equation (30). Using the modes determined in Section 4.1.2 to find $d\theta/d\eta$, the solutions for the various cases are as follows.

(a) $\tau = \Gamma = 0$ From equation (23)

$$\theta = A \sin \frac{\pi}{2} \eta = \theta_o \frac{\sin \frac{\pi}{2} \eta}{\sin \frac{\pi}{2} \eta_o}$$

therefore

$$\frac{d\theta}{d\eta} = A \frac{\pi}{2} \cos \frac{\pi}{2} \eta$$

and

$$U_d = \frac{GJ_m}{2s} \left(\frac{\theta_o}{\sin \frac{\pi}{2} \eta_o} \cdot \frac{\pi}{2} \right)^2 \int_o^1 \cos^2 \frac{\pi}{2} \eta \cdot d\eta$$

$$= \frac{GJ_m}{16s} \frac{\pi^2 \theta_o^2}{\sin^2 \frac{\pi}{2} \eta_o} \qquad (37)$$

(b) $\tau = 0$, $\Gamma \neq 0$ From equation (24) writing

$$\zeta = (1 - \Gamma\eta) \quad \text{then} \quad \zeta_o = (1 - \Gamma\eta_o) \quad \text{and} \quad \beta = \frac{K}{\Gamma}$$

we have

$$\theta = AJ_o(\beta\zeta) + BY_o(\beta\zeta) = Z_o(\beta\zeta)$$

therefore

$$\frac{d\theta}{d\zeta} = \beta Z_{-1}(\beta\zeta) = -\beta Z_1(\beta\zeta)$$

and

$$U_d = \int_o^1 \frac{1}{2} \frac{GJ}{s} \left(\frac{d\theta}{d\eta} \right)^2 d\eta$$

$$= -\frac{GJ_m \beta^2 \Gamma}{s(2 - \Gamma)} \int_1^{(1-\Gamma)} \zeta \left\{ Z_1(\beta\zeta) \right\}^2 d\zeta \; . \qquad (38)$$

Solution of this integral can be expressed as

$$U_d = -\frac{GJ_m \beta^2 \Gamma}{s(2-\Gamma)} \left[\frac{\zeta^2}{2} \left\{ [Z_1(\beta\zeta)]^2 - Z_o(\beta\zeta)\, Z_2(\beta\zeta) \right\} \right]_1^{(1-\Gamma)}$$

$$= -\frac{GJ_m \beta^2 \Gamma}{s(2-\Gamma)} \left[\frac{(1-\Gamma)^2}{2} \left\{ [Z_1(\beta-K)]^2 - Z_o(\beta-K)\, Z_2(\beta-K) \right\} \right.$$

$$\left. - \frac{1}{2} \left\{ [Z_1(\beta)]^2 - Z_o(\beta)\, Z_2(\beta) \right\} \right] .$$

This expression presents some difficulties in determining U_d as the values of the constants A and B are different for each reference section. However from Section 4.1.2 and the Appendix the ratio of the constants has been determined. Writing

$$Z_o = \left\{ \frac{A}{B} J_o(\ ) + Y_o(\ ) \right\} B , \qquad Z_1 = \{\ \}\, B \quad \text{etc.}$$

where

$$B = \frac{\theta_o}{\frac{A}{B} J_o(\beta\zeta_o) + Y_o(\beta\zeta_o)} \tag{39}$$

we can write the expression for the dynamic strain energy as

$$U_d = \left\{ -\frac{GJ_m \beta^2 \Gamma}{2(2-\Gamma)} \left[\frac{(1-\Gamma)^2}{2} \left\{ [Z_1(\beta-K)]^2 - Z_o(\beta-K)\, Z_2(\beta-K) \right\} \right. \right.$$

$$\left. \left. - \frac{1}{2} \left\{ [Z_1(\beta)]^2 - Z_o(\beta)\, Z_2(\beta) \right\} \right] \right\} \frac{\theta_o^2}{\{Z_o(\beta\zeta_o)\}^2} \tag{40}$$

where the expression inside the brackets $\{\ \}$ reduces to a single value for a particular wing and the variation with the choice of reference section is incorporated in the term B^2 equation (39).

(c) $\tau \neq 0$, $\Gamma = 0$ This is treated in a similar manner to 7.2(b), when, from equation (25), making the substitution $\zeta = (1 - \tau\eta)$, $\beta = K/\tau$ we have

$$\theta = \zeta^{-1} Z_1(\beta\zeta)$$

and

$$\frac{d\theta}{d\zeta} = -\beta\zeta^{-1} Z_2(\beta\zeta)$$

whence

$$U_d = \int_0^1 \frac{1}{2} \frac{GJ}{s} \left(\frac{d\theta}{d\eta}\right)^2 d\eta = \int_1^{(1-\tau)} \frac{1}{2} \frac{GJ}{s} \left(\frac{d\theta}{d\zeta}\right)^2 d\zeta(-\tau)$$

$$= -\frac{4\, GJ_m\, \beta^2 \tau}{s(2-\tau)^3} \left[\frac{(1-\tau)^2}{2} \left\{ [Z_2(\beta-K)]^2 - Z_1(\beta-K)\, Z_3(\beta-K) \right\} \right.$$

$$\left. - \frac{1}{2} \left\{ [Z_2(\beta)]^2 - Z_1(\beta)\, Z_3(\beta) \right\} \right]$$

whence expressing

$$Z_1 = \left\{ \frac{A}{B} J_1(\ ) + Y_1(\ ) \right\} B \ , \quad Z_2 = \left\{\ \right\} B \quad \text{etc.}$$

where

$$B = \frac{\theta_o}{\zeta_o^{-1} Z_1(\beta\zeta_o)} = \frac{\theta_o}{\zeta^{-1} \left\{ \frac{A}{B} J_1(\beta\zeta_o) + Y_o(\beta\zeta_o) \right\}} \qquad (41)$$

we have

$$U_d = -\frac{4\, GJ_m\, \beta^2\, \tau}{s(2-\tau)^3} \left[\frac{(1-\tau)^2}{2} \left\{ [Z_2(\beta-K)]^2 - Z_1(\beta-K)\, Z_2(\beta-K) \right\} \right.$$

$$\left. - \frac{1}{2} \left\{ [Z_2(\beta)]^2 - Z_1(\beta)\, Z_3(\beta) \right\} \right] \frac{\theta_o^2\, \zeta_o^2}{\{Z_1(\beta\zeta_o)\}^2}$$

... (42)

(d) $\tau = \Gamma \neq 0$ The equation (26) by a similar substitution to 7.1.2(b) can be written as

$$\theta = \zeta^{-3/2} Z_{3/2}(\beta\zeta)$$

whence

$$\frac{d\theta}{d\zeta} = -\beta\zeta^{-3/2} Z_{5/2}(\rho\zeta)$$

and the expression for the strain energy becomes

$$U_d = -\frac{8\,GJ_r\,\beta^2\tau}{s(2-\tau)^4}\left[\frac{(1-\tau)^2}{2}\left\{[Z_{5/2}\,(\beta-K)]^2 - Z_{3/2}\,(\beta-K)\,Z_{7/2}\,(\beta-K)\right\}\right.$$

$$\left. -\frac{1}{2}\left\{[Z_{5/2}\,(\beta)]^2 - Z_{3/2}\,(\beta)\,Z_{7/2}\,(\beta)\right\}\right] . \qquad (43)$$

The evaluation of U_d was hampered by the lack of suitable tables. In order to overcome this the Bessel function obtained for $d\theta/d\eta$ was expressed as trigonometry ratios and then the integration for the dynamic strain energy was performed graphically. To reduce the work to a minimum we wrote

$$Z_{5/2} = \left\{\frac{A}{B}J_{5/2} + Y_{5/2}\right\}B \quad \text{where} \quad B = \frac{\theta_o\,\zeta_o^{3/2}}{Z_{3/2}(\beta\zeta_o)} .$$

Hence for the numerical case considered

$$U_d = 59078\left\{\frac{\theta_o\,\zeta_o^{3/2}}{\sqrt{\frac{2}{\pi\beta\zeta_o}}\left[\frac{A}{B}\left\{\frac{\sin\beta\zeta_o}{\beta\zeta_o} - \cos\beta\zeta_o\right\} - \left\{\sin\beta\zeta_o + \frac{\cos\beta\zeta_o}{\beta\zeta_o}\right\}\right]}\right\}^2$$

7.3 Numerical examples

The ratio of the strain energies U_s/U_d is obtained from the two preceding sections and as the twist of the reference section is the same in the two modes this ratio is also the ratio of the static stiffness to the dynamic stiffness m_θ/m'_θ . The results obtained are plotted, in Fig.11, against the spanwise co-ordinate η, and show that an increase in skin taper produces a reduction in the stiffness ratio, the effect being most marked at the tip. For rectangular wings the peak of m_θ/m'_θ moves from $\eta = 0.8$ to $\eta = 0.6$ for skin taper variation of $-2 \leq \Gamma \leq 1$ and falls from 0.955 for $\Gamma = -2$ to 0.86 for $\Gamma = 1$. The effect of wing taper is similar to that obtained in Ref.1. The variation of m_θ/m'_θ with skin taper at reference section $\eta = 0.7$ is shown in Fig.12. For rectangular wings the effect of skin taper is slight with $\Gamma < 2/3$, but for $\Gamma > 2/3$ the reduction is more marked. For a tapered wing the reduction in m_θ/m'_θ in the range $0 \leq \Gamma \leq 2/3$ is greater than for a rectangular wing in the case considered ($\tau = 2/3$). In Fig.13 are plotted the dynamic mode and the static mode for reference section at $\eta = 0.7$ and $\eta = 1.0$ for the tapered wing with skin taper ($\tau = \Gamma = 2/3$). It can be seen that the difference in strain energy is appreciable.

8 CONCLUSIONS

The main conclusion to be drawn from the present report is that the effect of skin taper on the divergence, flutter, and aileron reversal speeds is not large when the comparison is made on the basis of constant wing weight.

For a rectangular wing, skin taper leads to a slight increase in divergence, flutter, and reversal speeds, whereas skin inverse taper leads to a slight decrease. The opposite effect is obtained for a tapered wing with a tip chord to root chord ratio of 1 : 3.

The effect of skin taper on the ratio of the static stiffness to the dynamic stiffness is small for rectangular wings in the realistic range of skin taper for a reference section at 0.7 semi-span. For tapered wings the effect is more pronounced, the stiffness ratio diminishing as the skin taper is increased.

A comparison of the calculated flutter speeds (found using two-dimensional derivatives) with speeds found from flutter criteria shows that the trends of variation of calculated speed with skin taper agree closely with those predicted by a criterion based upon static stiffness. A criterion based upon strain energy in a linear twist mode shows trends contrary to those given by calculation.

NOTATION

a_1	aerodynamic coefficient $\frac{dC_L}{d\alpha}$
a_2	aerodynamic coefficient $\frac{dC_L}{d\beta}$ where β is the aileron rotation angle
c	wing chord ft
C	defined in text
d	distance from wing root to equivalent tip (0.9s)
e	distance between flexural axis and aerodynamic centre as fraction of the chord
E	ratio of aileron chord to wing chord
f	flutter frequency c.p.s.
g	position of inertia axis aft of L.E. as fraction of chord
GJ	torsional rigidity at a section
h	position of flexural axis aft of L.E. as fraction of chord
I	value of inertia at a section / unit length
k	ratio of tip chord to root chord
K	defined in text
ℓ_ϕ	flexural stiffness as measured at reference section lb ft/rad

NOTATION (Contd)

m	aerodynamic coeff. $\frac{dC_m}{d\beta}$
m_θ	torsional stiffness as measured at reference section lb ft/rad
M	free stream Mach number
M_1	free stream Mach number corresponding to speed V_1
p	fundamental wing torsional freq. c.p.s.
r	stiffness ratio $\left(= \frac{\ell_\phi}{d^3} \Big/ \frac{m_\theta}{dc_m^2}\right)$
s	wing semi-span (root to tip) ft
t	skin thickness
u	defined in text
U	strain energy in a linear torsion mode, torsion about the centre-line of the box with an amplitude of one radian at the tip (lb ft)
V	critical speed ft/sec
V_c	critical flutter speed as used in criterion
V_D	design diving speed (M cos $\Lambda \leq 1$) knots E.A.S.
V_2	final estimated flutter speed as used in criterion
x	chordwise coordinate (a/t of reference axis)
y	spanwise coordinate
z	downward displacement
α	wing incidence radians
β	angle of sweepback of wing flexural axis radians
Γ	skin taper = $(1 - t_{tip}/t_{root})$
ζ	$(1 - \tau\eta)$ or $(1 - \Gamma\eta)$ as defined in text
η	non-dimensional spanwise coordinate
θ	wing twist
Λ	sweepback leading edge radians

NOTATION (Contd)

ρ air density ρ_o = density sea level (0.002378 slugs/ft^3)

ρ_w wing density $\left(= \dfrac{\text{mass of one wing}}{s\, c_m^2}\right)$ slugs/ft^3

σ_w wing relative density $= \dfrac{\text{density of wing}}{\text{density of surrounding air}}$

τ wing taper $(1 - k) = \left(1 - \dfrac{c_T}{c_R}\right)$

AR aspect ratio

Subscripts

m refers to value at the mean chord position

r refers to value at the mean chord position when t_m is varied

T refers to value at the tip

R refers to value at the root

0 refers to value of expression when $\tau = \Gamma = 0$

LIST OF REFERENCES

No.	Author(s)	Title, etc
1	Collar, A.R., Broadbent, E.G., Puttick, E.B.	An elaboration of the criterion for wing torsional stiffness. A.R.C. R.& M. 2154. January, 1946.
2	Collar, A.R., Broadbent, E.G.	Rolling power of an elastic wing. A.R.C. R. & M. 2186. October, 1945.
3	Broadbent, E.G.	The estimation of wing divergence speed. A.R.C. R. & M. 2288. December, 1945.
4	Molyneux, W.G.	Flutter of wings with localised masses. R.A.E. Report Structures 214. J.R.Ae.Soc., Vol.61, No.10, p 667. October, 1957.
5	Duncan, W.J., Collar, A.R., Lyon, H.M.	Oscillations of elastic blades and wings in an airstream. A.R.C. R. & M. 1716. January, 1936.

LIST OF REFERENCES (Contd)

No.	Author(s)	Title, etc
6	Timoshenko, S.	Vibration problems in engineering. 1937. D Van Nostrand Co. Inc.
7	Walker, P.B.	Simple formulae for the fundamental natural frequencies of cantilevers. A.R.C. R. & M. 1831. July, 1937.
8	Templeton, H.	The technique of flutter calculations. A.R.C. C.P.172. April, 1953.
9	Minhinnick, I.T.	Subsonic aerodynamic flutter derivatives for wings and control surfaces (compressible and incompressible flow). A.R.C. 14,228, 14,855. July, 1950.
10	Molyneux, W.G., Ruddlesden, F.	Flutter tests on some delta wings using ground launched rockets. A.R.C. R. & M. 3231. February, 1955.
11	Broadbent, E.G.	The elementary theory of aero-elasticity. Bunhill Publications.

APPENDIX 1

Calculation of divergence speed and mode for $\tau = 2/3$, $\Gamma = 0$.

From equation (14) we have the solution as

$$f = (1 - \tau\eta)^{-1} \left\{ AJ_2 \left(2 \frac{u}{\tau} \sqrt{1 - \tau\eta} \right) + BY_2 \left(2 \frac{u}{\tau} \sqrt{1 - \tau\eta} \right) \right\} \qquad (44)$$

where

$$u^2 = \frac{\rho V^2 (2 - \tau)\, ea_1\, c_m^2\, s^2}{4\, G J_m}$$

writing

$$\frac{u}{\tau} = \gamma \quad \text{and} \quad (1 - \tau\eta) = \zeta$$

and putting equation (44) in the form

$$f = \zeta^{-1} Z_2(2\gamma\zeta^{1/2}) = \zeta^{-1} \left\{ AJ_2(2\gamma\zeta^{1/2}) + BY_2(2\gamma\zeta^{1/2}) \right\} .$$

This equation must satisfy the end conditions

(i) $f = 0$ when $\eta = 0$

(ii) $\frac{df}{d\eta} = 0$ when $\eta = 1$

From (i) $0 = Z_2(2\gamma)$ if $(1 - \tau\eta) \neq 0$.

Also

$$\frac{df}{d\eta} = - \gamma\zeta^{-3/2} Z_3(2\gamma\zeta^{1/2}) .$$

From (ii)

$$0 = Z_3(2\gamma \sqrt{1 - \tau}) \text{ if } (1 - \tau\eta) \neq 0 .$$

Now have two equations of the form

$$AJ_2(2\gamma) + BY_2(2\gamma) = 0 \qquad (45)$$

and

$$AJ_3(2\gamma \sqrt{1 - \tau}) + BY_3(2\gamma \sqrt{1 - \tau}) = 0 . \qquad (46)$$

For variable V we have, with the other terms being constant.

V	$J_2(2\gamma)$	$Y_2(2\gamma)$	$\frac{A}{B} = \left(-\frac{Y_2}{J_2}\right)$	$J_3(2\gamma\sqrt{1-\bar{\tau}})$	$Y_3(2\gamma\sqrt{1-\bar{\tau}})$	$\frac{A}{B} = \left(-\frac{Y_3}{J_3}\right)$
1000	0.41324	0.14685	-0.35537	0.15931	-0.95951	6.02289
1200	0.20584	0.33391	-1.62222	0.23088	-0.69691	2.91744
1400	-0.05231	0.35491	6.78493	0.31881	-0.51770	1.62383
1600	-0.25209	0.21742	0.86248	0.39577	-0.36106	0.93595
1800	-0.31215	-0.00329	-0.01054	0.42671	-0.20718	0.48553

Plotting $\frac{A}{B}$ against the speed V in Fig. 14 we get V ≑ 1580 ft/sec for the condition that $\frac{A}{B}$ is the same for both equation (45) and (46). Replotting for a narrower band of V (say 1550 < V < 1600) we find that V = 1581.4 ft/sec for a value of $\frac{A}{B}$ ≑ 0.9875.

Substituting this value of V back into equations (45) and (46) we have a check on the value of $\frac{A}{B}$. From (45) $\frac{A}{B}$ = 0.98742. From (46) $\frac{A}{B}$ = 0.98738.

The value of $\frac{A}{B}$ was taken as 0.9874. The mode is given by equation (44). Taking unit displacement at a reference section (say f = 1 at η = 1) the values of A and B can be determined and hence the mode shape.

The method is essentially the same for the other solutions. In the torsion case the frequency p was taken as the variable.

TABLE 1

Wing properties

Semi-span s	2 ft
Chord c	$\frac{2(1-\tau n)}{(2-\tau)}\, c_m$
Mean chord c_m	1 ft
Flexural axis aft of wing L.E.	0.3c
Inertia axis aft of wing L.E.	0.45c
Radius of gyration of wing section about flexural axis	0.287c
Wing mass	0.0952 slugs
Mass of uniform rectangular wing per ft run, m_o	0.0476 slugs/ft
Uncoupled fixed root	
Bending frequency ($\tau = \Gamma = 0$)	16 c.p.s.
Torsion frequency ($\tau = \Gamma = 0$)	50 c.p.s.

TABLE 2

Numerical calculations

	Divergence speed ft/sec	Flutter				Aileron reversal speed ft/sec
		Speed ft/sec	Freqn. c.p.s.	Flexure c.p.s.	Torsion c.p.s.	
(a) $\tau = \Gamma = 0$	1017.8	475.1	33.1	16	50	534.1
(b) $\tau = 0$ $\Gamma \neq 0$						
$\Gamma = 1$	1101.3	492.3	66.2	32.2	76.55	568.7
$\Gamma = 2/3$	1094.0	498.1	45.9	21.7	61.09	568.4
$\Gamma = -2$	878.2	425.7	25.3	11.4	39.84	467.9
(c) $\tau \neq 0$ $\Gamma = 0$						
$\tau = 2/3$	1581.2	739.7	60.0	27.1	85.10	823.8
(d) $\tau = \Gamma \neq 0$						
$\tau = \Gamma = 2/3$ (const. t)	1562.7 1626.5	703.1	74.3	35.3	97.64	803.3

TABLE 3

Comparison of criterion and calculated flutter speeds (ft/sec)

	Modified calculated speed	Molyneux criterion speed	Broadbent criterion speeds	
			V_D	V_F
(a) $\tau = \Gamma = 0$	529.9	537.0	472.6	579.6
(b) $\tau = 0$ $\Gamma \neq 0$				
$\Gamma = 1$	547.6	557.2	457.6	561.6
$\Gamma = 2/3$	553.5	554.6	464.6	570.0
$\Gamma = -2$	478.6	497.8	485.1	594.6
(c) $\tau \neq 0$ $\Gamma = 0$				
$\tau = 2/3$	790.1	725.9	581.1	709.3
(d) $\tau = \Gamma \neq 0$				
$\tau = \Gamma = 2/3$	755.6	709.6	615.5	750.1

W.T.2078 C.P.642 K3. Printed in England.

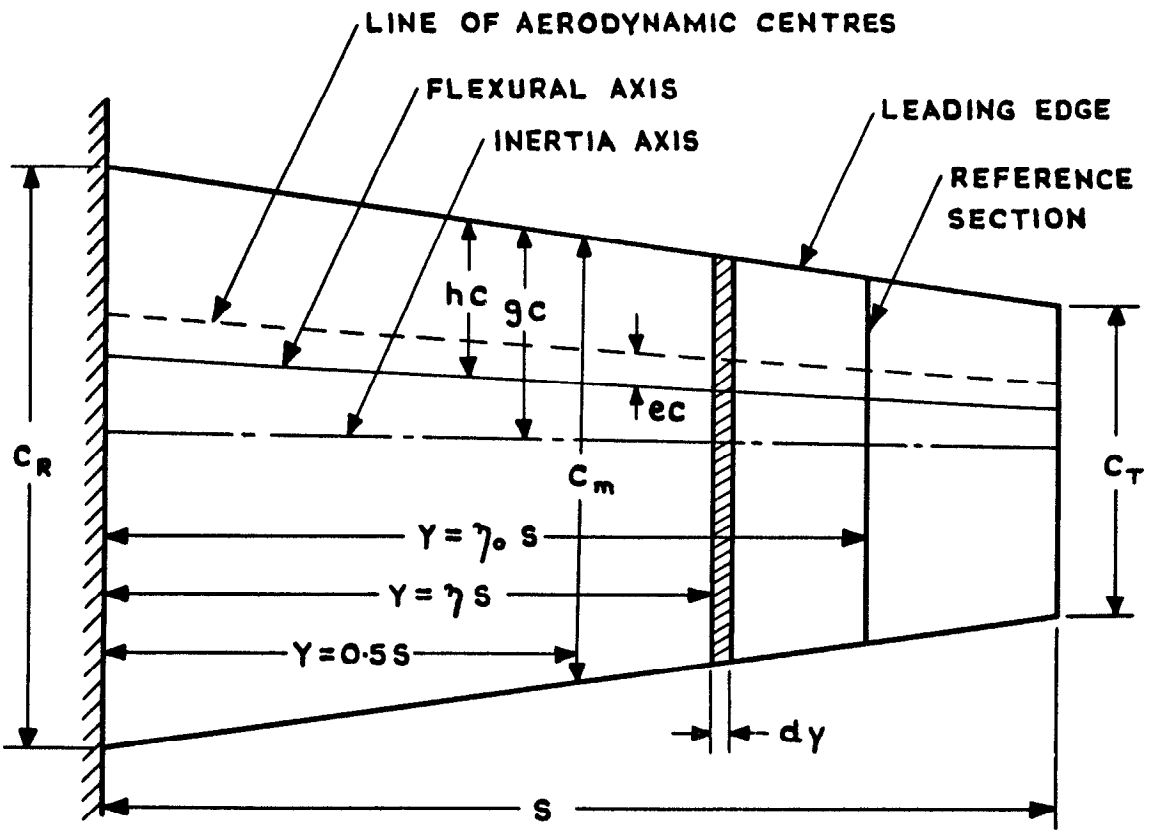

FIG. 1. DIAGRAM OF TAPERED WING.

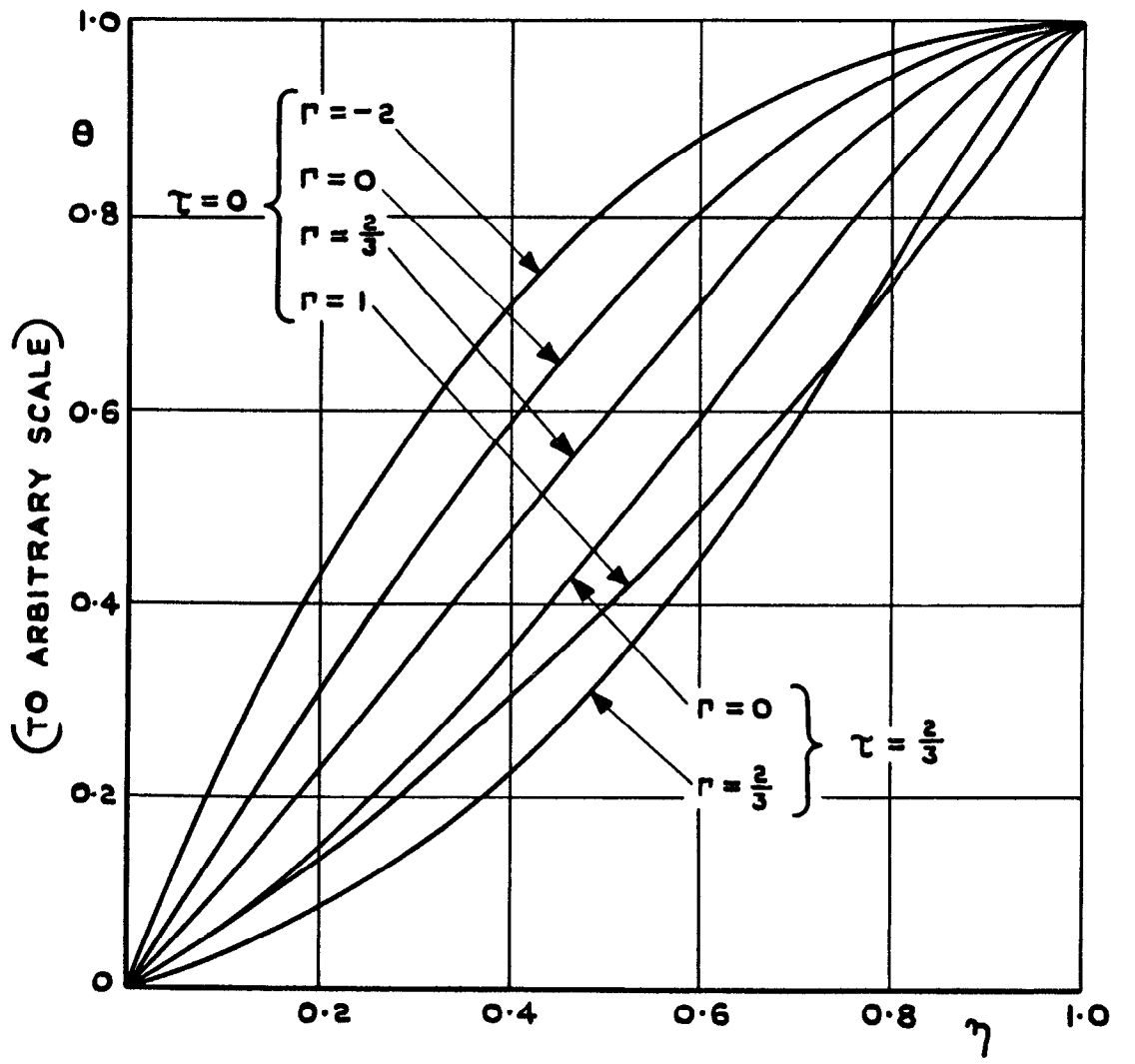

FIG. 2. DIVERGENCE MODES.

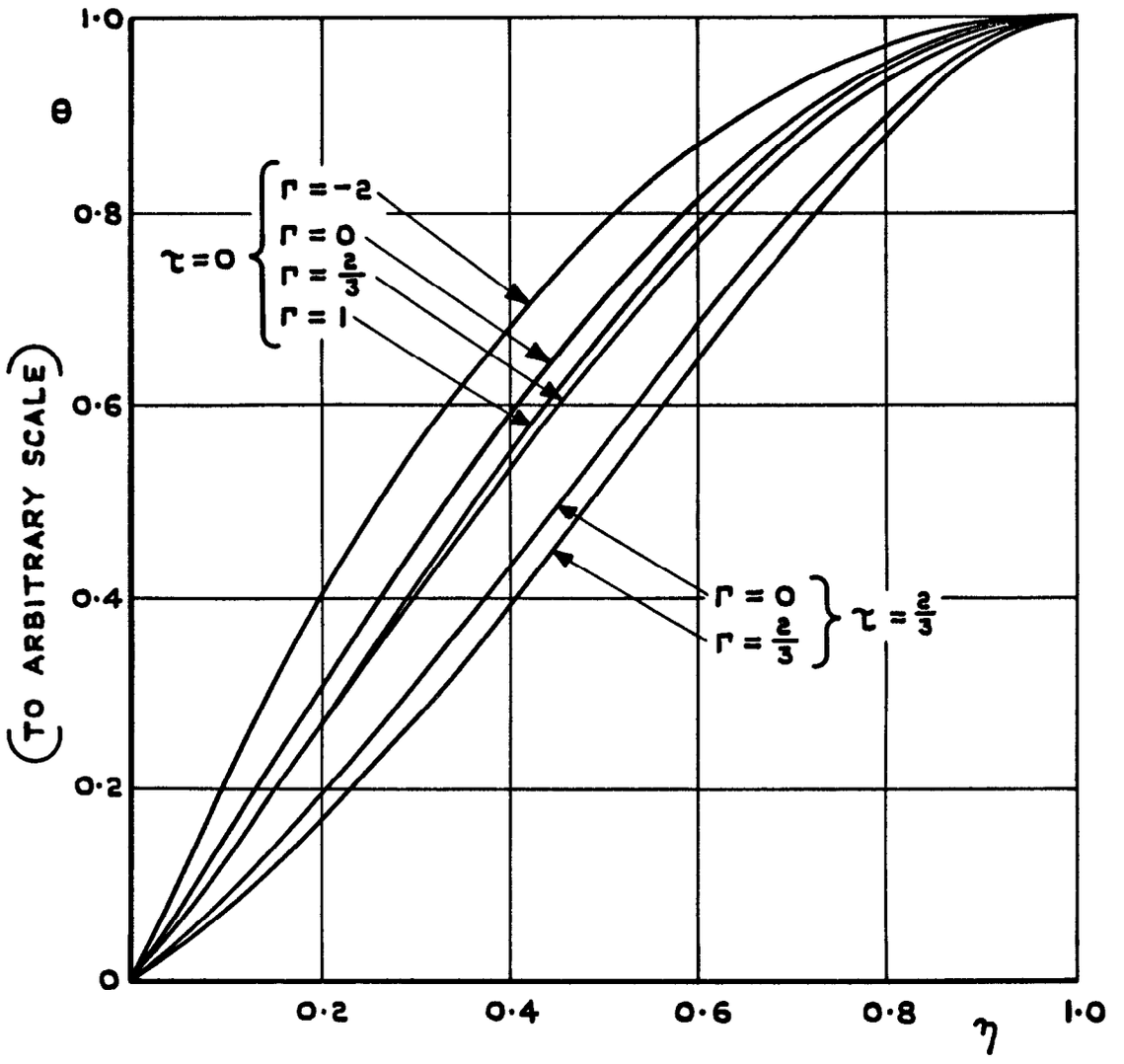

FIG. 3. FUNDAMENTAL TORSIONAL MODES.

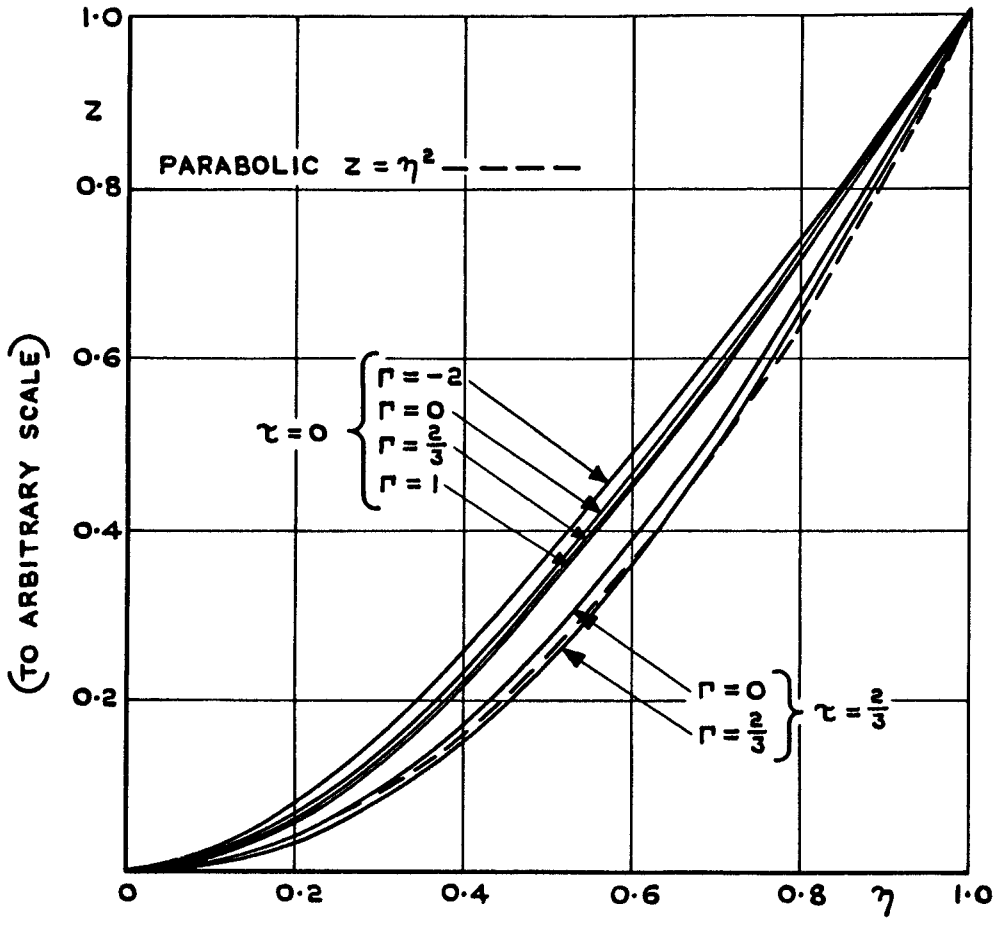

FIG. 4. FUNDAMENTAL FLEXURAL MODES.

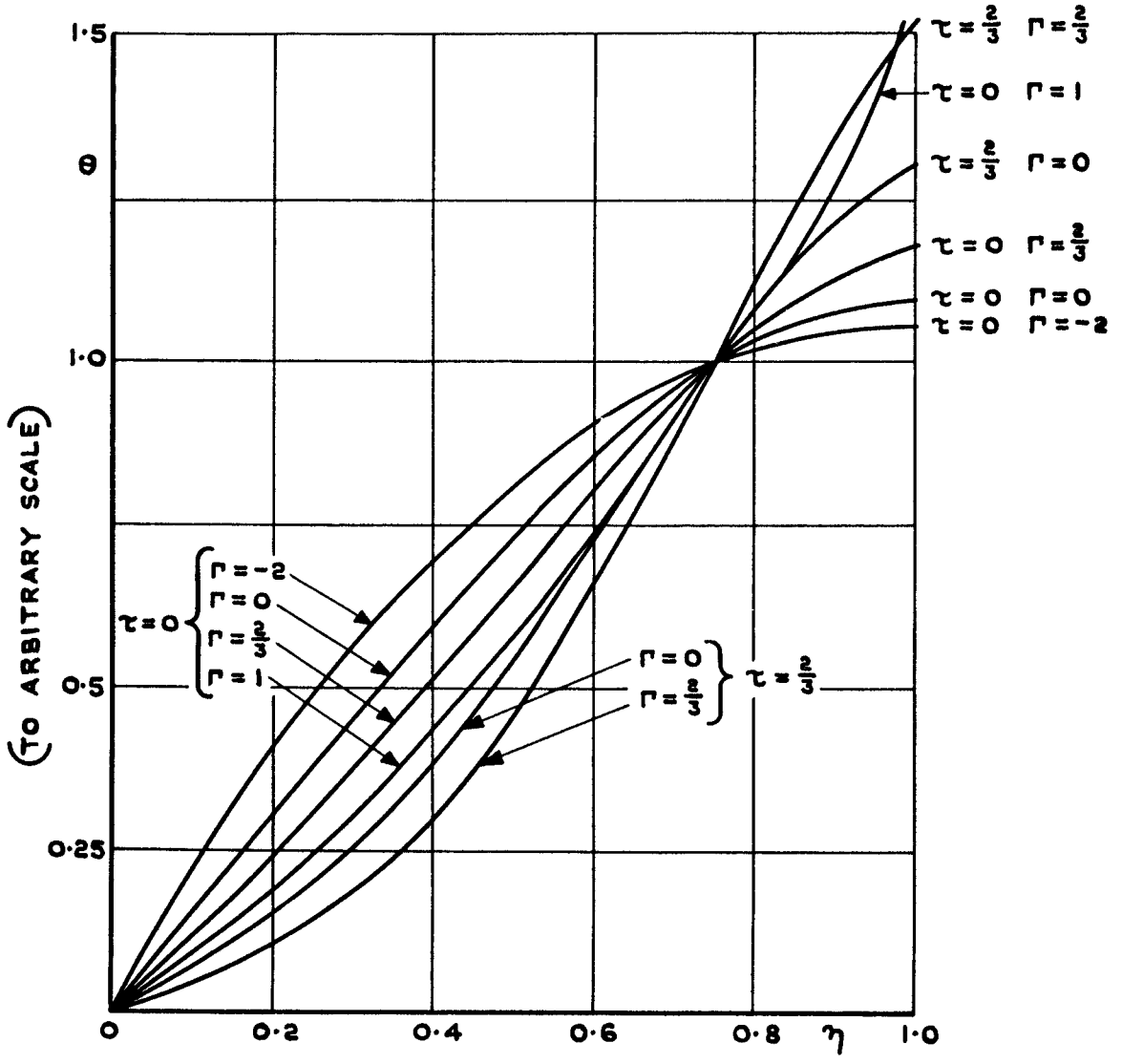

FIG. 5. AILERON REVERSAL MODES.

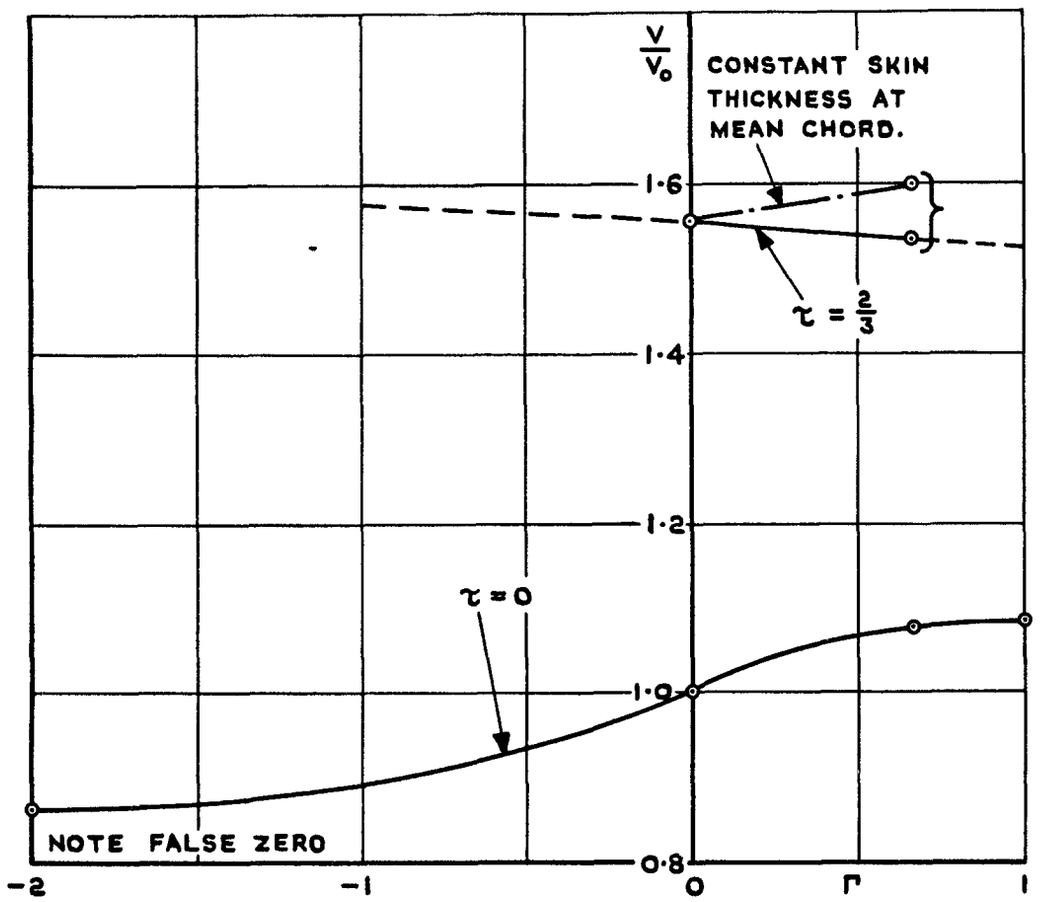

FIG. 6. VARIATION OF DIVERGENCE SPEED WITH SKIN TAPER.

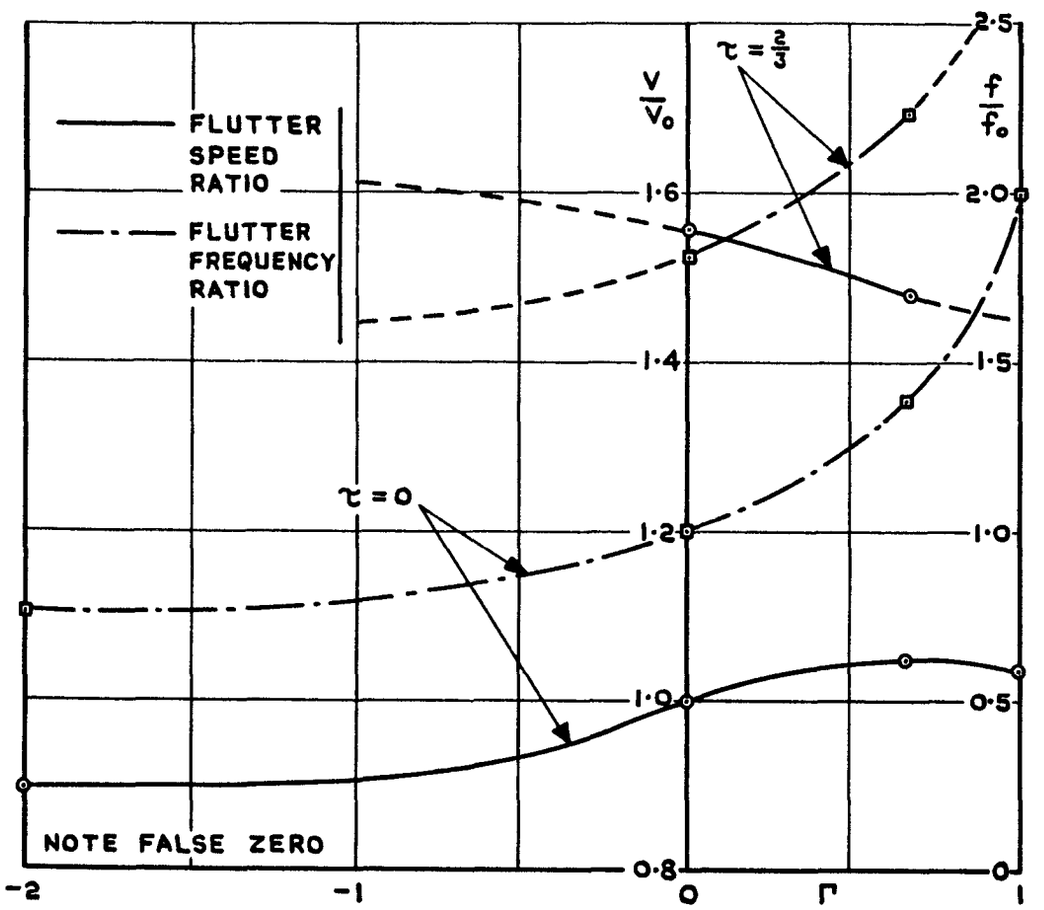

FIG. 7. VARIATION OF CRITICAL FLUTTER SPEED AND FREQUENCY RATIOS WITH SKIN TAPER.

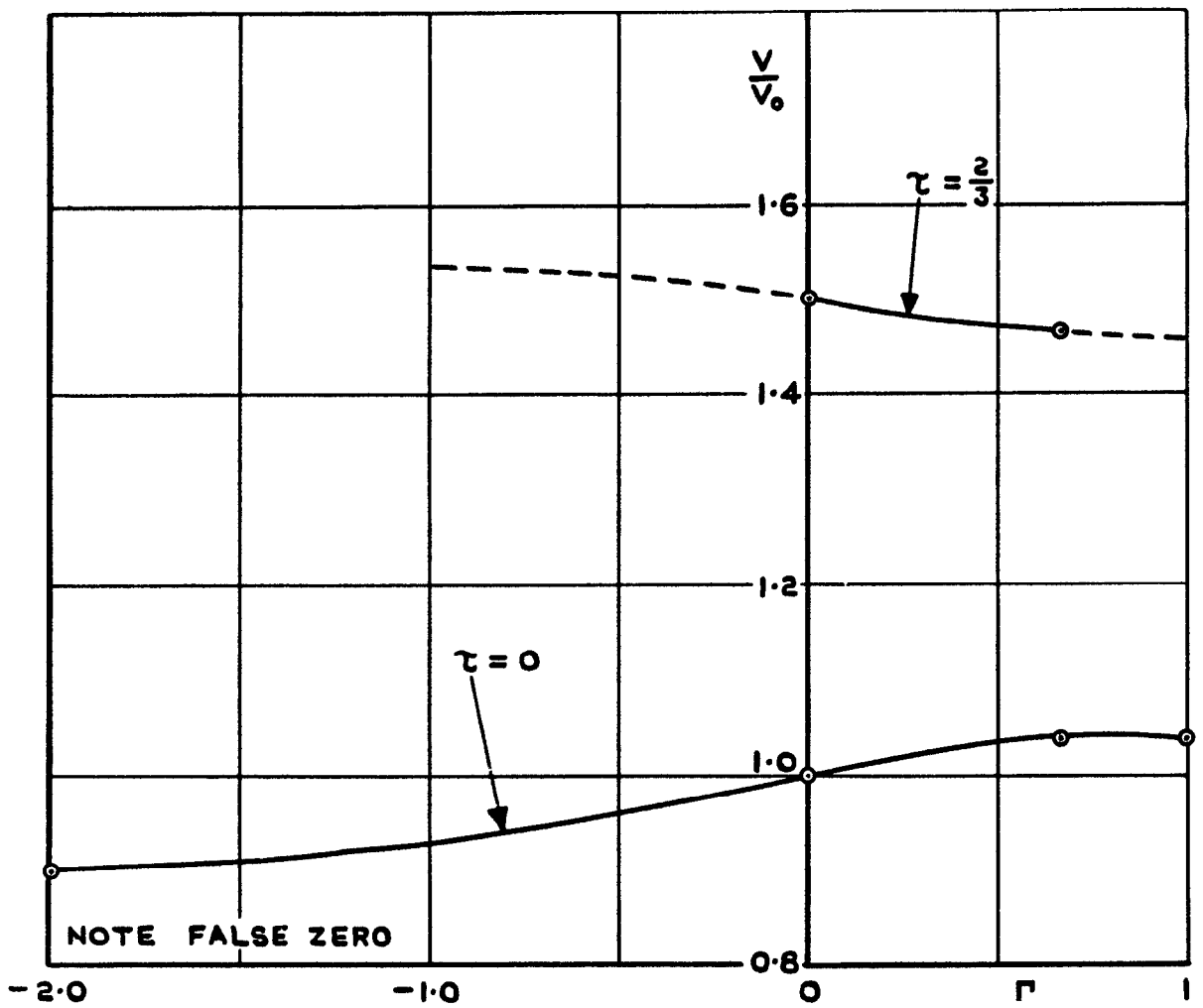

FIG. 8. VARIATION OF AILERON REVERSAL SPEED WITH SKIN TAPER.

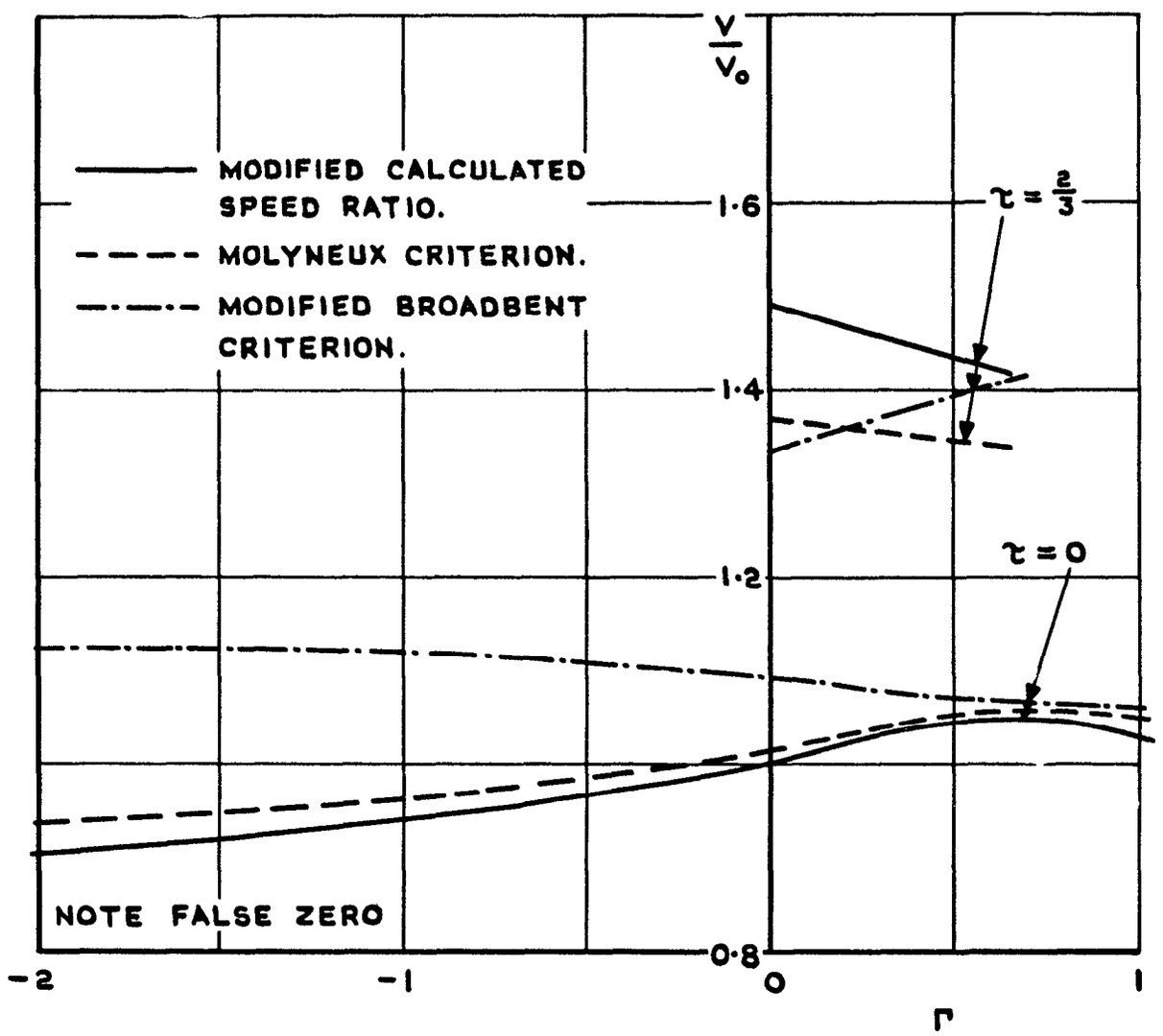

FIG. 9. COMPARISON OF FLUTTER SPEEDS OBTAINED FROM CRITERIA AND CALCULATION.

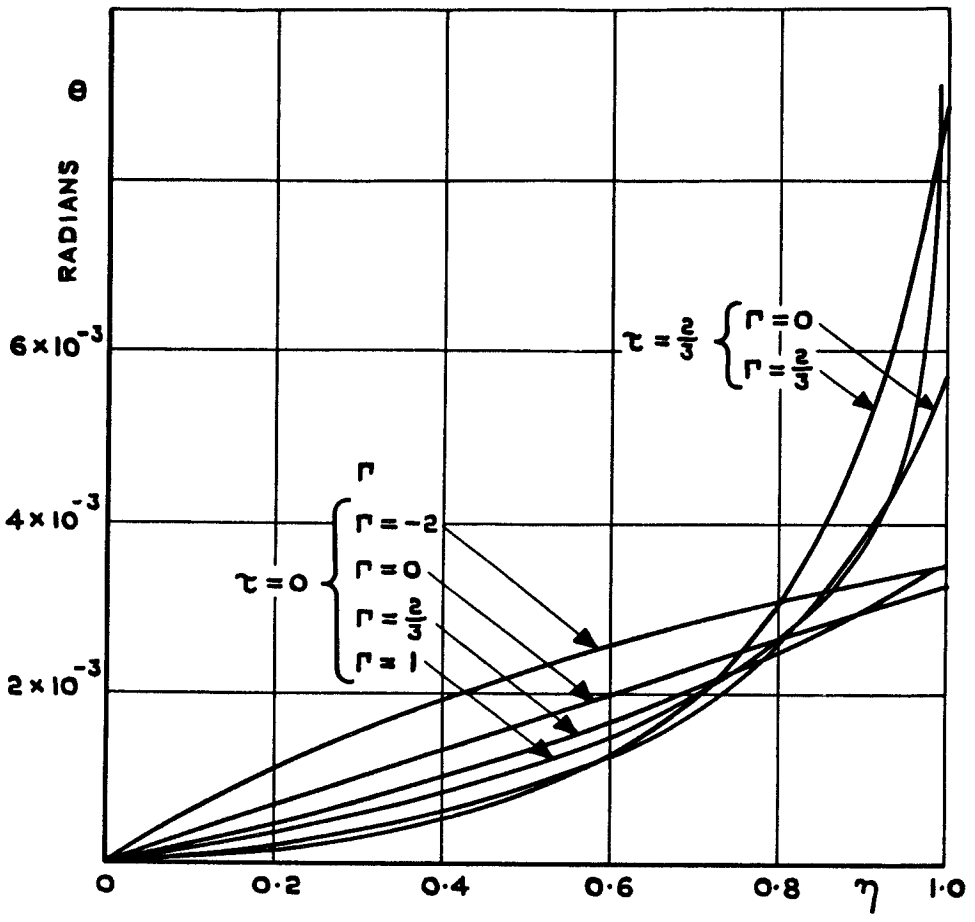

FIG. 10. STATIC TORSIONAL MODES FOR UNIT TORQUE AT TIP ($\eta = 1{\cdot}0$).

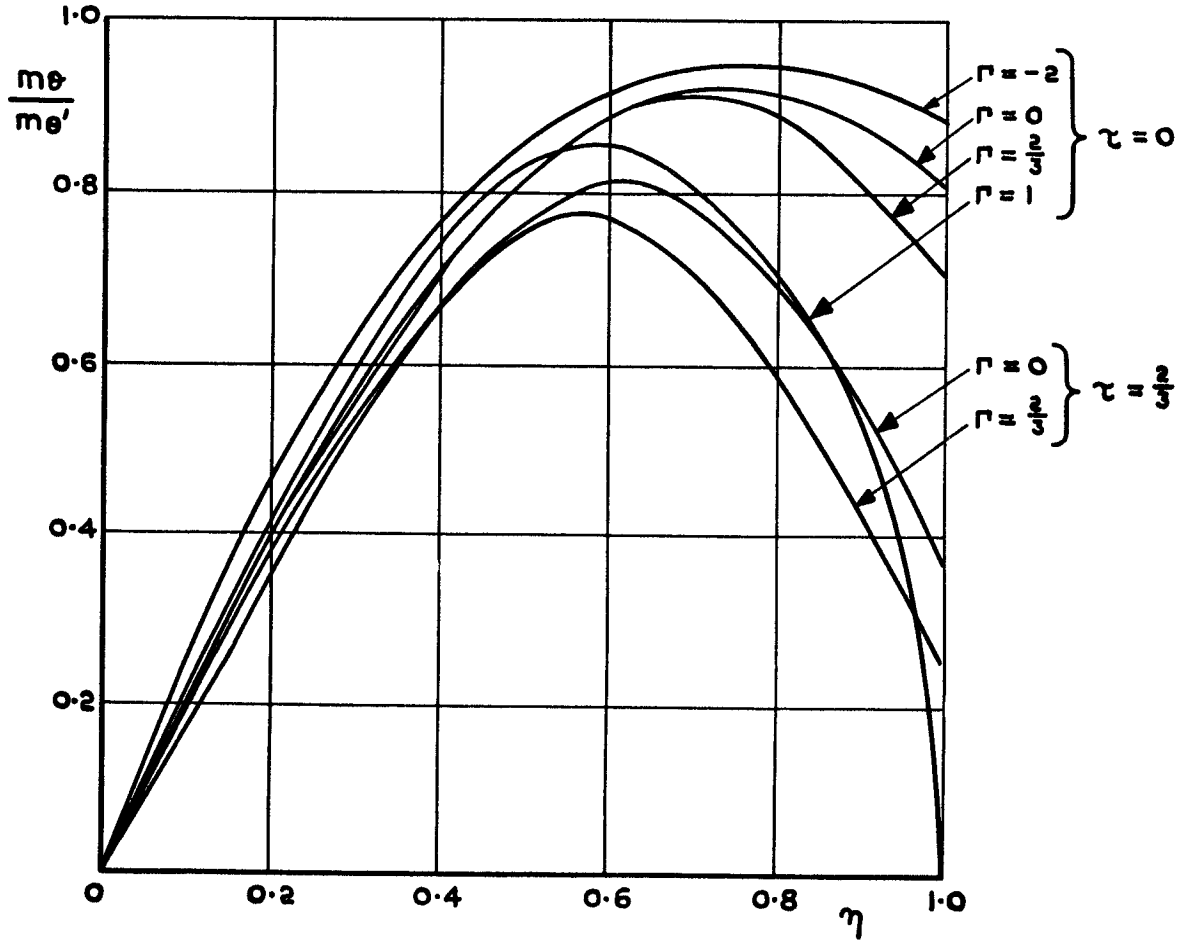

FIG. 11. VARIATION OF STIFFNESS WITH REFERENCE SECTION.

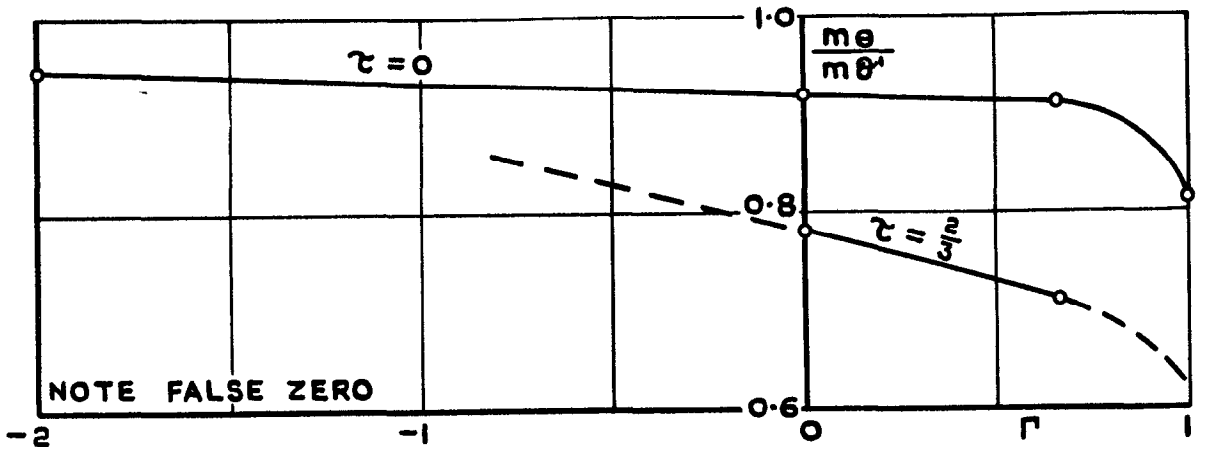

FIG. 12. VARIATION OF STIFFNESS WITH SKIN TAPER AT REFERENCE SECTION 0·7S.

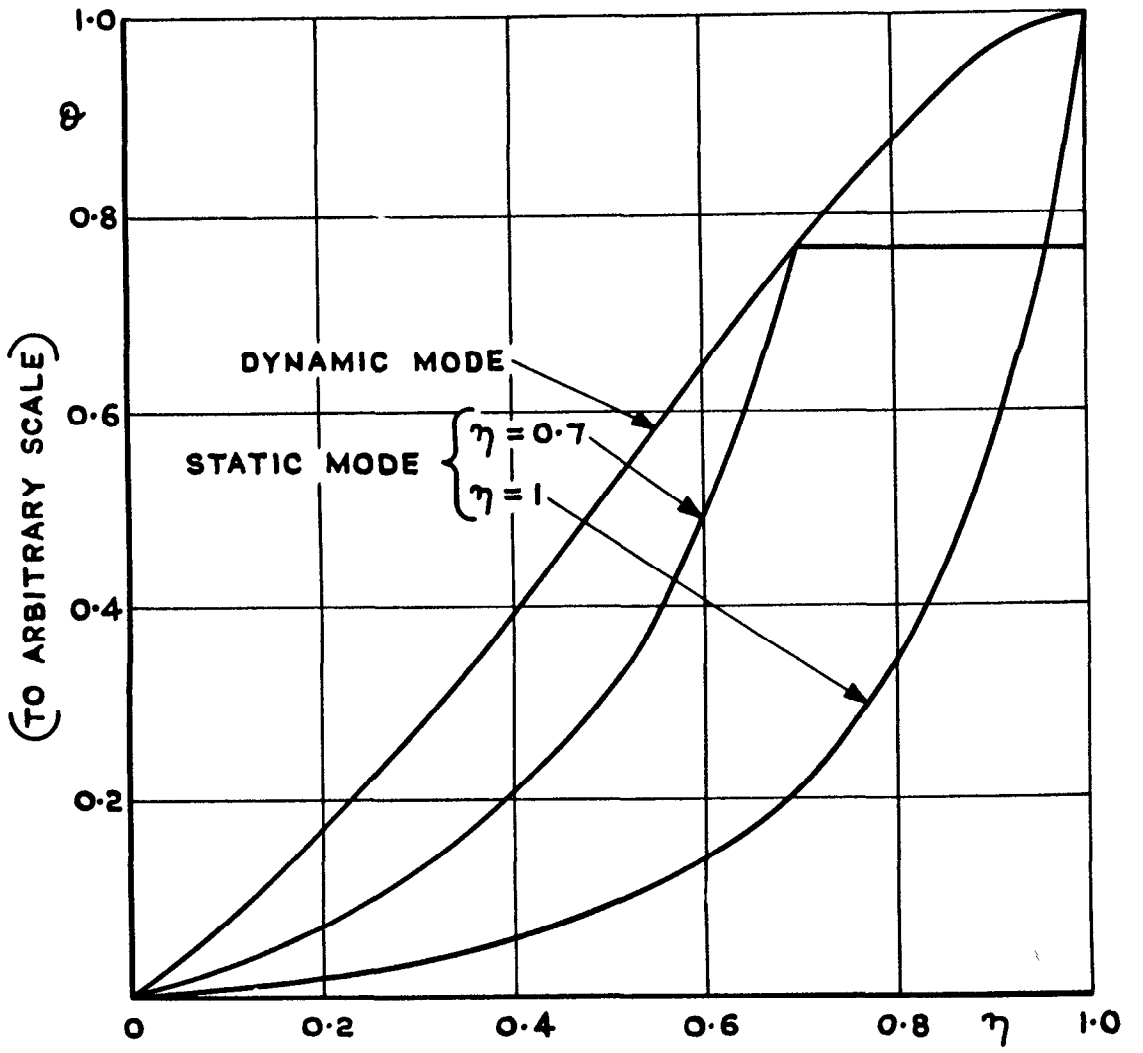

FIG. 13. STATIC AND DYNAMIC TORSIONAL MODES FOR $\tau = \Gamma = \frac{2}{3}$.

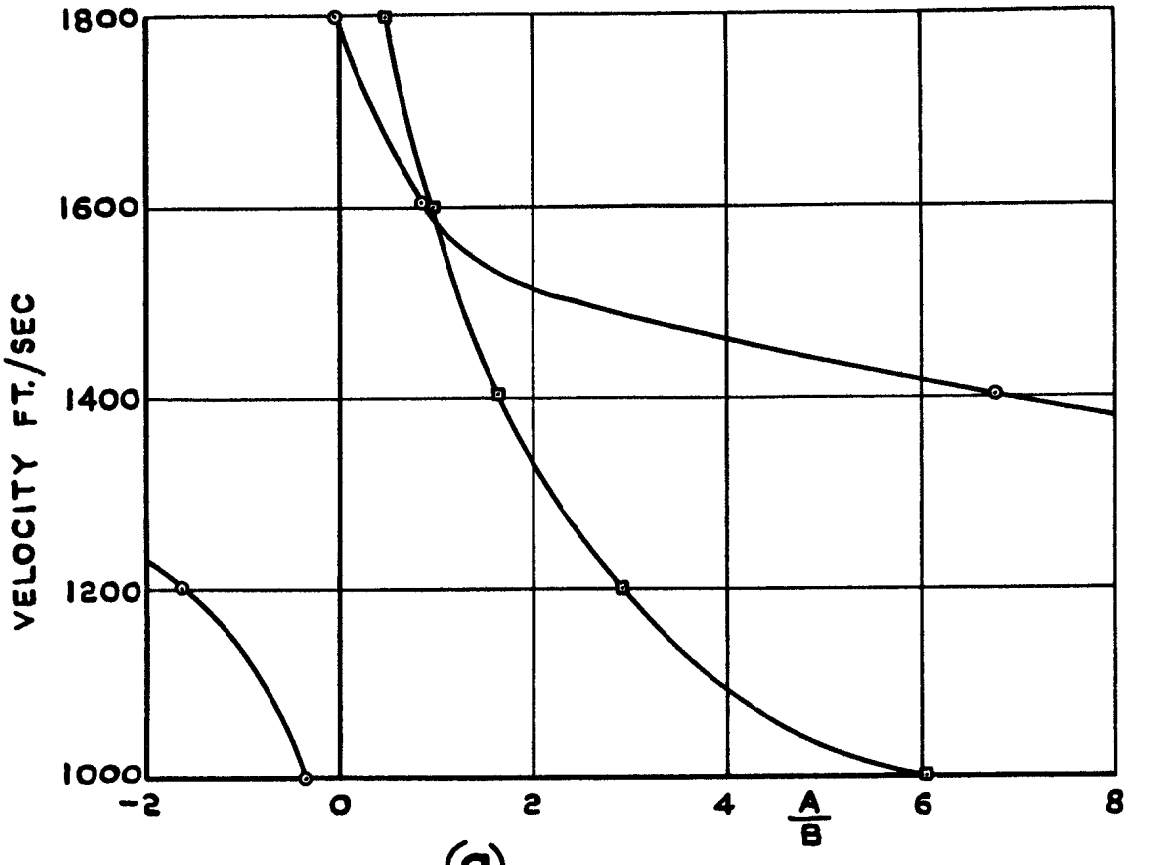

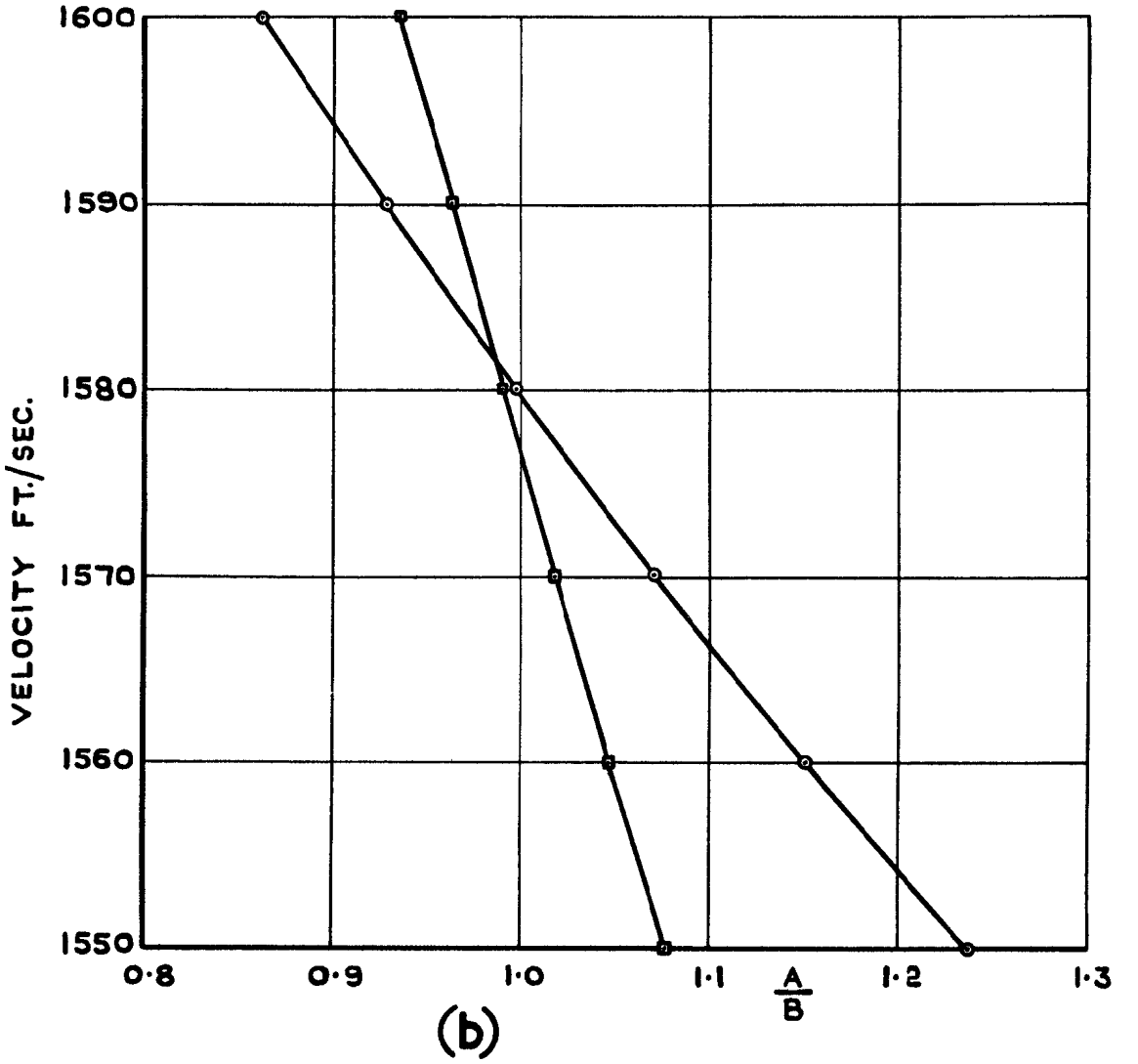

FIG. 14(a & b). DETERMINATION OF DIVERGENCE SPEED $\tau = \frac{2}{3}$ $\Gamma = 0$.

A.R.C. C.P. No.642

533.6.013.412 :
629.13.012.612

THE EFFECT OF SKIN TAPER ON THE AEROELASTIC PROPERTIES OF WINGS. Rein, J. A. March, 1961.

An analysis is made of the effect of linear variation of the spanwise skin thickness on the divergence, flutter, and aileron reversal speeds of thin wings.

It is assumed that the wing weight and stiffness are provided by the skin alone and that the wing mass remains constant for the tapers considered.

It is shown that for rectangular wings, a skin thickness tapering from root to tip produces an increase of up to 8% in the critical speeds,

(Over)

A.R.C. C.P. No.642

533.6.013.412 :
629.13.012.612

THE EFFECT OF SKIN TAPER ON THE AEROELASTIC PROPERTIES OF WINGS. Rein, J. A. March, 1961.

An analysis is made of the effect of linear variation of the spanwise skin thickness on the divergence, flutter, and aileron reversal speeds of thin wings.

It is assumed that the wing weight and stiffness are provided by the skin alone and that the wing mass remains constant for the tapers considered.

It is shown that for rectangular wings, a skin thickness tapering from root to tip produces an increase of up to 8% in the critical speeds,

(Over)

A.R.C. C.P. No.642

533.6.013.412 :
629.13.012.612

THE EFFECT OF SKIN TAPER ON THE AEROELASTIC PROPERTIES OF WINGS. Rein, J. A. March, 1961.

An analysis is made of the effect of linear variation of the spanwise skin thickness on the divergence, flutter, and aileron reversal speeds of thin wings.

It is assumed that the wing weight and stiffness are provided by the skin alone and that the wing mass remains constant for the tapers considered.

It is shown that for rectangular wings, a skin thickness tapering from root to tip produces an increase of up to 8% in the critical speeds,

(Over)

whereas an inverse taper results in a reduction of up to 14%. For a tapered wing, skin thickness tapering from root to tip results in a reduction in the critical speeds of up to 7%.

A comparison is made between the results obtained from the analysis and from some flutter speed criteria. Further the effect of skin taper on the mode of distortion and on the dynamic torsional stiffness is investigated.

whereas an inverse taper results in a reduction of up to 14%. For a tapered wing, skin thickness tapering from root to tip results in a reduction in the critical speeds of up to 7%.

A comparison is made between the results obtained from the analysis and from some flutter speed criteria. Further the effect of skin taper on the mode of distortion and on the dynamic torsional stiffness is investigated.

Published by
HER MAJESTY'S STATIONERY OFFICE

To be purchased from
York House, Kingsway, London w.c.2
423 Oxford Street, London w.1
13A Castle Street, Edinburgh 2
109 St. Mary Street, Cardiff
39 King Street, Manchester 2
50 Fairfax Street, Bristol 1
35 Smallbrook, Ringway, Birmingham 5
80 Chichester Street, Belfast 1
or through any bookseller

Printed in England

S.O. CODE No. 23-9013-42